AFML-TR-66-259

INVESTIGATION OF PRECIPITATES IN TWO CARBON-CONTAINING COLUMBIUM-BASE ALLOYS

F. OSTERMANN
AIR FORCE MATERIALS LABORATORY

and

F. BOLLENRATH
INSTITUTE OF TECHNOLOGY, AACHEN

TECHNICAL REPORT AFML-TR-66-259

DECEMBER 1966

AIR FORCE MATERIALS LABORATORY
RESEARCH AND TECHNOLOGY DIVISION
AIR FORCE SYSTEMS COMMAND
WRIGHT-PATTERSON AIR FORCE BASE, OHIO

NOTICES

When Government drawings, specifications, or other data are used for any purpose other than in connection with a definitely related Government procurement operation, the United States Government thereby incurs no responsibility nor any obligation whatsoever; and the fact that the Government may have formulated, furnished, or in any way supplied the said drawings, specifications, or other data, is not to be regarded by implication or otherwise as in any manner licensing the holder or any other person or corporation, or conveying any rights or permission to manufacture, use, or sell any patented invention that may in any way be related thereto.

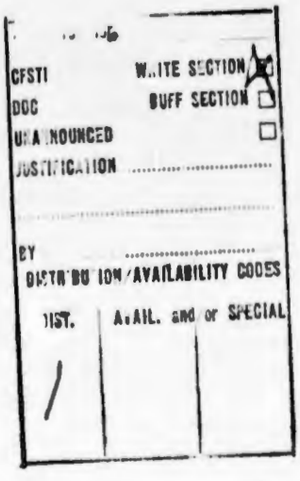

Copies of this report should not be returned to the Research and Technology Division unless return is required by security considerations, contractual obligations, or notice on a specific document.

900 - March 1967 - C0192-26-584

AFML-TR-66-259

INVESTIGATION OF PRECIPITATES IN TWO CARBON-CONTAINING COLUMBIUM-BASE ALLOYS

F. OSTERMANN
AIR FORCE MATERIALS LABORATORY

and

F. BOLLENRATH
INSTITUTE OF TECHNOLOGY, AACHEN

FOREWORD

The work reported here was conducted in the laboratory of the Strength and Dynamics Branch, Metals and Ceramics Division, Air Force Materials Laboratory, Wright-Patterson Air Force Base, Ohio from July 1963 to September 1965. The program was initiated under Project No. 7351, "Metallic Materials", Task No. 735106, "Behavior of Metals". The work was performed by Mr. F. Ostermann of Air Force Materials Laboratory with Professor Dr. F. Bollenrath of Institute of Technology, Aachen, Germany as advisor.

The investigation was undertaken by Mr. Ostermann in partial fulfillment of requirements for the degree of Doctor of Engineering Sciences at Institute of Technology, Aachen.

Mr. John Gerhardstein, University of Dayton, assisted in the experimental work throughout the course of the program. Thanks are extended to Mrs. K. Branch, University of Cincinnati, for her help in performing the precipitate phase extractions.

The authors express their gratitude to Mr. Walter J. Trapp for his continued encouragement and support.

The manuscript was released by the authors May 30, 1966 for publication as a Research Technology Division Technical Report.

This technical report has been reviewed and is approved.

W. J. TRAPP
Chief, Strength and Dynamics Branch
Metals and Ceramics Division

ABSTRACT

The precipitates in the commercial columbium alloys D-31 and D-43 were investigated after various heat treatments. The titanium-rich and zirconium-rich monocarbides are the only stable precipitate phases in alloys D-31 and D-43, respectively. The temperatures for complete solid solution are 1600°C for alloy D-31 and 1700°C for alloy D-43 corresponding to a carbon content of about 0.09 wt.-%. Non-equilibrium columbium carbides precipitate even during quenching from solid solution, so that no appreciable carbon supersaturation can be achieved in columbium alloys. During aging, the stable monocarbides form at the expense of the non-equilibrium columbium carbides but not from solid solution. Therefore, age-hardening caused by stable MC-phase precipitation does not occur. The effect of oxygen on carbide precipitates was investigated by increasing the oxygen concentration of the alloys on purpose. Oxygen behaved differently in both alloys with respect to precipitate phases. A columbium carbide phase with unknown lattice structure but a composition corresponding approximately to Cb_3C_2 was found in both alloys after suitable heat treatments.

TABLE OF CONTENTS

ILLUSTRATIONS

ILLUSTRATIONS (CONTINUED)

TABLES

SECTION I

INTRODUCTION

1.1 PURPOSE AND OBJECTIVE

During an investigation of the weldability of some columbium alloys, it became necessary to obtain more precise information about the precipitation reactions which occur in the fusion and heat-affected zones. Interpretation of results of a heat treatment study conducted for this purpose indicated disagreement with results of previous investigators. Consequently this investigation was conducted to study the precipitation reactions in carbon-containing columbium alloys more extensively and to reconsider the results of previous investigations. As experimental material, two commercial columbium alloys were selected which have the same carbon content but different types and concentrations of metallic alloying elements. By comparing the behavior of the two alloys, it was hoped to point out the general as well as the particular influence of the alloying elements on the precipitation reactions and to give some consideration to the role which oxygen plays in the formation of the precipitates in these alloys.

1.2 BACKGROUND

Small impurity amounts of carbon, nitrogen, and oxygen generally cannot be avoided in fabrication of commercial columbium-base alloys. The total amount of these elements is usually 0.05 percent* or less. However, even such small amounts can cause precipitates due to the low solubility of these elements in columbium.

The maximum solubility of carbon in columbium is reported by Pochon et al (Reference 1) with 0.03% at 2235°C. Elliott (Reference 2) and Kimura and Sasaki (Reference 3), however, find a larger maximum solubility of 0.8 percent at the same temperature. The solubility decreases rapidly with decreasing temperature to approximately 0.1% at 1800°C (Reference 2). The results of Begley and co-workers (Reference 4) agree with those of Elliott and suggest a solubility of less than 0.01% at 1200°C.

Nitrogen is more soluble in columbium than is carbon. The investigations of Albrecht and Goode (Reference 5) and Elliott and Komjathy (Reference 6) yield solubilities of 0.8% and 0.25% at 1800° and at 1200°C, respectively. The results of Cost and Wert (Reference 7), deLamotte, Huang, and Altstetter (Reference 8), and Gebhard, Fromm, and Jakob (Reference 9) are in agreement at 1500°C (0.42%) with those of Albrecht-Goode and of Elliott-Komjathy. However, they find a somewhat faster decrease of the solubility of nitrogen with decreasing temperature. In an earlier investigation of the columbium-nitrogen system by the internal friction method Ang and Wert (Reference 10) found also a smaller solubility at low temperatures than did Albrecht and Goode (0.036% at 800°C).

The solid solubility of oxygen in columbium is also larger than that of carbon. Elliott (Reference 11) reports a solubility of 0.25% at 500°C and of 0.72% at the eutectic temperature (1915°C).

*All concentrations are given in weight percent unless otherwise noted.

By adding metallic alloying elements the solubility of oxygen in columbium can be changed considerably. The addition of molybdenum and tungsten will probably decrease the solubility for interstitial elements because of the smaller atomic radii. Owing to the higher affinity of oxygen, additions of zirconium also cause a decrease of the solubility limit. Hobson (Reference 12) finds only a solubility of 0.03 percent oxygen in a Cb-1Zr alloy at 1600°C, and Barber and Morton (Reference 13) determine the solubility of oxygen in the same alloy with 0.01% at 1000°C.

A similarly large effect of zirconium addition on the solubility of nitrogen in columbium was not found in the few reported investigations. DeLamotte, Huang, and Altstetter (Reference 14) find no essential shift of the solubility limit in columbium between 1500° and 2100°C for zirconium contents of 0.86 percent and 1.5 percent. However, since the ratio of nitrogen to zirconium in this temperature region is large, deLamotte et al. point out that an influence of zirconium may be found perhaps at higher Zr-concentrations.

As a result of the relatively small solubilities of oxygen, nitrogen, and also carbon, most commercial columbium alloys contain precipitate phases which can influence the behavior of these alloys during fabrication and application. If a fine particle size can be maintained, precipitate phases may have a beneficial effect on strength at high temperatures. This, however, is largely not found for columbium alloys developed so far. Hobson (Reference 12) finds a strength maximum for Cb-1Zr alloy (0.021%C, 0.014%O, 0.016%N) after solution annealing (1600°C/2hrs.) and subsequent aging for 50 hrs. at 927°C. Further aging at 927°C causes a decrease in strength. This is in agreement with results by Stewart, Liebermann, and Rowe (Reference 15) who made hardness measurements on the same alloy after annealing at 1760°C and aging at 927°C. The precipitation hardening in these columbium-zirconium alloys was thought to be due to zirconium oxide, although an influence of nitrides and carbides was not excluded. Chang (Reference 16) also reports rapid overaging in Cb-1Zr alloy (0.02%O, 0.01%N, 0.005%C) at 955°C. A precipitation hardening effect at higher temperatures, however, was found by Chang in the columbium alloy F-48 (Cb-14.7%W-5.5%Mo-1%Zr- 0.10%C, 0.033%N, 0.028%O). After solution annealing at 1925°C and 2200°C a hardness peak was found by aging for 1 hr at 1200°C. Rapid overaging occurred above 1200°C. The age-hardening was thought to be due to the precipitation of Zr-rich (Zr,Nb)C. In the same investigation Chang also found precipitation hardening in the columbium alloy F-50 (Cb-13.8%W-4.85%Mo-4.37%Ti-0.9%Zr-0.035%C,0.023%O, 0.031%N). The hardness peak in this alloy, however, was already found after aging for 1 hr at 982°C and was apparently caused by the precipitation of (Zr,Nb,Ti)C. The high titanium concentration was probably responsible for the lower range of stability of the precipitate. According to Begley and co-workers (Reference 4) small additions of oxygen to Cb-5Hf and Cb-5Hf-1Ti-1Zr alloys gave improved strength properties at 1100°C. The precipitate phases in these alloys were mainly hafnium oxide. Simultaneous additions of oxygen and nitrogen to Cb-5Zr (Reference 17) and Cb-5Hf (References 17 and 18) alloys had a more pronounced effect on the hot-hardness in the temperature region below 1200°C than equal or higher amounts of oxygen or nitrogen alone (Reference 17). Coagulation of precipitates in nitrogen- and oxygen-containing Cb-Hf alloys occurred around 950° to 1000°C after aging for 1 hr (Reference 18). In nitrogen-containing Cb-Hf alloys embrittlement was, however, encountered in the solution annealed condition (1800°C) (Reference 18). The precipitation reaction was apparently caused by the formation of hafnium nitride (Reference 18). Additions of carbon to Cb-Hf and Cb-Zr alloys caused a less prominent precipitation hardening (Reference 17): however, the ductility of these alloys was not affected.

In summary then, it can be stated that in columbium alloys containing zirconium, hafnium, or titanium precipitation hardening is apparently generated by formation of nitrides, oxides, and carbides, which improve the strength at higher temperatures to some extent. Compared to carbon- or oxygen-containing alloys the addition of nitrogen in concentrations of 0.1 to 0.2 reduce the cold ductility in the solution annealed condition. However, in many cases the

observed precipitation processes cannot be ascribed clearly to either nitrogen, oxygen, or carbon, since these elements are almost always simultaneously present and interaction of these elements in the precipitation reaction cannot be excluded. These investigations of precipitation hardening phenomena in columbium alloys have shown that the stability of the precipitate phases, which have beneficial effects on high temperature strength, is limited to temperatures below 1000° or 1100°C, which is not sufficient in view of the intended service temperatures for these alloys of 1200°C or higher.

Chang (Reference 16) points out the temperature regions for the columbium alloys F-48 and F-50 in which the various precipitates are stable. According to his investigations three different precipitates are of importance in the columbium alloy F-48. A (Zr, Cb)C is stable in temperature regions up to 1600°C, Cb_2C between 1600° and 2200°C, and ZrO_2 between 1600° and 2100°C. Therefore, annealing the alloy F-48 at temperatures between 1800° and 2000°C causes precipitation of Cb_2C and ZrO_2. If such sample is subsequently annealed at 1300°C both Cb_2C and ZrO_2 are dissolved and the mixed carbide (Zr, Cb)C, which possibly also contains oxygen and nitrogen, precipitates. In the columbium alloy F-50 which in comparison to F-48 contains approximately 5 percent titanium and somewhat less carbon (0.035%), formation of Cb_2C is suppressed. Chang's results (Reference 16) consequently suggest that the solid solubility of carbon in F-48 and F-50 is extremely low even at elevated temperatures, so that complete solid solution may be achieved only at temperatures close to the melting point of the alloys. This interpretation is accepted by Yount and Keller (Reference 19) in an investigation of the columbium alloy D-43 (Cb-10%W-1%Zr-0.1%C, 0.02%O, 0.007%N). After annealing the alloy D-43 for 1 hr at 2345°C they observed a single-phase structure. Begley et al. (Reference 17) find in the carbon-containing Cb-5Hf and Cb-5Zr alloys that as in the F-50 alloy (Reference 16) the formation of Cb_2C is suppressed by the high Hf- and Zr-concentrations and that the monocarbides are "stabilized" up to at least 2000°C.

One can argue against these interpretations that a drastic reduction of carbon solubility by relatively minor additions of metallic alloying elements like Zr, Hf, or Ti is unlikely from analogy to the Cb-Zr-N system. Assuming that the carbon solubility in columbium is not reduced, then the stability of some of the observed precipitates must be questioned. An alternate interpretation of the experimental results would be that some of the precipitates, observed after high-temperature annealing, have formed during cooling. This interpretation assumes a very rapid rate of precipitation, which is supported by the observation of carbide precipitates in the fusion zone of electron-beam welds in relatively thin sheet of the columbium alloy D-43 (Reference 19). These precipitates have obviously formed during the rapid cooling from the melt.

SECTION II

EXPERIMENTAL MATERIALS

As experimental materials for this investigation, two commercial columbium alloys were selected which have a nominal carbon content of 0.1 percent and are different in the type and concentration of the carbide forming elements. Alloy D-31 contains 10 percent (approx. 17 at.-%) titanium, alloy D-43 only 1 percent (approx. 1 at.-%) zirconium.

Chemical analysis, producer and process history are given below in Sections 2.1 and 2.2. Since both alloys were received in the annealed condition, a sample was taken from each sheet and cold-rolled 50 percent on a two-high rolling mill for the purpose of determining the temperature regions for recovery from cold-work

2.1 COLUMBIUM ALLOY D-31

Received as sheet of 0.041 inch thickness from Manufacturing Technology Division, Wright-Patterson Air Force Base. Producer: E. I. Du Pont De Nemours and Co., Wilmington, Del.
Charge Number: S-98726, sheet Nr. 3
Nominal Composition: Cb-10%Mo-10%Ti-0.1%C
Process History:

1. Hammer forged from 8" diameter ingot to 13.5" x 1.750" x 17.75" at 1290℃
2. Annealed 1 hour at 1370℃
3. Hot rolled from slab to sheet bar 16" x 0.781" x 21.25" at 1200℃
4. Annealed 1 hour at 1370℃
5. Hot rolled from sheet bar to mold out 29" x 0.300" x 35" at 1200℃
6. Annealed 1 hour at 1200℃
7. Hot rolled from mold out to hot rolled sheet 28" x 0.150" x 59" at 1200℃
8. Vacuum-annealed 1 hour at 1200℃
9. Cold rolled to 28.25" x 0.075" x 30.5"
10. Vacuum annealed 1 hour at 1200℃
11. Cold rolled to 28.5" x 0.041" x 54"
12. Vacuum annealed 1 hour at 1100℃

Chemical Analysis (by Ledoux & Co., Teaneck, N.J.):

Molybdenum	9.64%	Aluminum	20ppm
Titanium	8.43%	Copper	50ppm
Carbon	0.094%	Iron	70ppm
Oxygen	0.017%	Lead	70ppm
Nitrogen	0.013%	Silicon	50ppm
Hydrogen	1.4ppm	Tantalum	3500ppm
		Vanadium	10ppm
		Zirconium	20ppm

2.2 COLUMBIUM ALLOY D-43

Received as sheet of 0.030 inch thickness from Manufacturing Technology Division, Wright-Patterson Air Force Base. Producer; E. I. Du Pont De Nemours and Co., Wilmington, Del.
Charge Number: 43-387-2
Nominal Composition: Cb-10%W-1%Zr-0.1%C
Process History:

1. Extrusion of 8"diameter ingot to 2" x 6"x length sheet bar at 1100°C (steel casing)
2. Cross rolling to 1/4" plate at 1200°C
3. Flattened and conditioned
4. Annealed 1 hour at 1200°C
5. Cold rolled to 0.100" sheet
6. Annealed 1 hour at 1200°C
7. Cold rolled to penultimate gage
8. Solution heat treated for 10 minutes at 1650°C
9. Cold rolled to final gage
10. Annealed one hour at 1425°C
11. Flattened

Chemical Analysis:	by Producer:	by Ledoux & Co.
Tungsten	9.4%	9.04%
Zirconium	1.00%	0.96%
Carbon	0.1070%	0.097%
Oxygen	0.0136%	0.0067%
Nitrogen	0.0040%	0.0025%
Hydrogen	3ppm	-.-
Silicon	-.-	0.001%
Titanium	-.-	0.002%
Molybdenum	-.-	0.001%
others	-.-	not detected

SECTION III

EXPERIMENTAL PROCEDURES

3.1 HEAT TREATMENT

Compared to other materials the heat treatment of columbium and columbium alloys is a problem, since considerable reaction with gases occurs already at relatively low temperatures and large variations in properties are caused by minute differences in the gas content. Especially the absorption of oxygen, i.e. external and internal oxidation, plays an important role during annealing which in most cases is difficult to separate in the analysis of experimental results.

Only recently, attention has been focussed to the gas-metal reactions occurring during annealing of columbium alloys in conventional vacuum furnaces. However, the reported investigations are concerned without exception with long time tests at temperatures below 1200°C. No systematic results are known for vacuum annealing at higher temperatures. Internal oxidation effects below 1200°C are important for the heat treatment of columbium alloys, since recovery, recrystallization, and precipitation processes occur in this temperature region. Most investigations (References 20, 21, and 23) are concerned with the influence of vacuum on the properties and chemical composition of columbium and columbium-zirconium alloys as a function of temperature and annealing time. Inouye (Reference 20) compares the gas contents of columbium, tantalum, molybdenum, and columbium-zirconium alloys after annealing for 1000 hours between 600° and 1200°C in a vacuum of 2.7×10^{-7} Torr and finds that the absorption of gases, i.e. predominantly oxygen, by tantalum and molybdenum is relatively small compared to columbium. Also the absorption of gases by columbium-zirconium alloys is about 2 to 3 times as large as by unalloyed columbium under identical conditions. The investigations of Roche (Reference 23) are in agreement with those of Inouye, namely that a vacuum of better than 1×10^{-7} Torr is necessary for the prevention of gas absorption for longer annealing times. Hall and Titran (Reference 22) show that even with a vacuum of about 1×10^{-8} Torr a measurable increase of the oxygen concentration occurs in columbium alloys during long time annealing at temperatures between 1100° and 1200°C. Some prevention of gas absorption can, however, be achieved by wrapping the samples into metal foils (References 20 and 21). Although some scatter in the results is caused by differences in wrapping, this procedure limits the gas absorption to tolerable levels. The efficiency of Ta, Mo, W, and Cb-1Zr foils was approximately equal in these investigations. With the use of protective foils, acceptable results can be obtained at 1×10^{-6} Torr during 1000 hours annealing, at temperatures between 700° and 1200°C.

For the aging tests of the columbium alloys D-31 and D-43 in the temperature region up to 1100°C, a vacuum system was originally built which provided a minimum pressure of 6×10^{-6} Torr. During aging experiments with the alloy D-43, it was found that even at relatively short annealing times, at temperatures between 700° and 1000°C, considerable gas absorption occurred if no protective tantalum foil was used. Figure 1 shows the influence of annealing time between 900° and 1050°C on the hardness at room temperature. Curve A gives the hardness data for a single sample which was taken out of the furnace for the hardness measurements after certain times. The data for curves B and C, however, are from samples with a continuous heat treatment for the times indicated. For the samples of curves A and B no protective tantalum foils were used. The different hardness levels of curves A and B indicate a higher sample contamination by repeated initial degassing of the system (curve A) as compared to a single degassing (curve B). However, even one degassing may lead to oxidation

phenomena, since a much lower hardness is shown by curve C for samples with protective tantalum foils. Recovery or overaging processes do not occur in this case. These results made an improvement of the vacuum system necessary in order to prevent oxidation phenomena with greater certainty. With the modified vacuum system a minimum pressure of less than 5×10^{-7} Torr was obtained. In addition, the whole vacuum system was carefully degassed before each aging test. All samples used in this investigation were wrapped in tantalum foil, except where stated.

Heat treatment at temperatures above 1100°C was conducted in vacuum furnaces with tantalum heat elements which were arranged in radiation- and water-cooled vacuum chambers. Since it was necessary to obtain maximum cooling rates from very high temperatures, two different types of furnaces had to be used, the particularities of which in terms of vacuum and cooling rate will be described briefly.

The most frequently used high-temperature vacuum furnace ("A") provided a vacuum during annealing of 1×10^{-5} Torr. The maximum cooling rate of this furnace is plotted in Figure 2 and was obtained by radiation cooling only. The temperature was measured with a W/WRe thermocouple as well as by optical pyrometry. The precision of the temperature measurement is approximately ±1%. The thermocouple was not connected with the sample but was located in a tungsten "black body" within the hot zone. Within the experimental error the cooling curves for maximum cooling rate was identical after annealing at various high temperatures. The influence of type of material and mass of annealing samples on the cooling rate was not measured. However, the deviation seems to be negligibly small, since usually about the same amount of samples were annealed and the mass of the samples was comparatively small. The samples were wrapped into tantalum foil to prevent gas absorption during annealing. During the investigation it became desirable to obtain slower cooling rates. The vacuum furnace, the maximum cooling rate of which is plotted in Figure 2, permitted to program the cooling rate by a "Data-trak" (Research Incorporated). The different cooling rates used in this investigation are also plotted in Figure 2.

Since in some instances the maximum cooling rate which can be achieved by radiation cooling was not sufficient, a vacuum quenching furnace at Battelle Memorial Institute, Columbus, Ohio was used instead. After annealing in this furnace ("B") the sample is released by a mechanism and drops from the tantalum hot zone into an oil bath. The minimum pressure of this furnace, however, was limited to approximately 1×10^{-4} Torr. In order to obtain maximum and uniform quenching the samples were not wrapped into tantalum foil, so that a larger variation of gas content must be taken into consideration in the analysis of the results.

3.2 INTERNAL OXIDATION

In the course of the present investigation it became desirable to increase the oxygen content of some samples in order to determine the role which oxygen plays in the precipitation reactions in carbon-containing columbium alloys. The glass vacuum system, which was used for the aging tests, was particularly suited for these experiments, since columbium alloys absorb gases already at temperatures below 1000°C and since the heat elements were not oxidized due to the external heating of the quartz furnace tube. Because a precision mercury pressure gage was not available, the amount of the absorbed gases was measured directly by measuring the weight difference of the sample. Pure oxygen was fed into the evacuated system after the high vacuum valve was closed. In order to reproduce the gas amount in the system from test to test, the gas was leaked into the system and measured with a thermocouple gage until a pressure of approximately 25×10^{-3} Torr was obtained. The initial pressure was maintained at this low level in order to prevent the formation of external oxide films. The gas was fed into the unheated system. The samples were subsequently annealed at 900°C and the pressure drop was monitored by the thermocouple pressure gage.

3.3 METALLOGRAPHY AND HARDNESS TESTING

For the metallographic preparation the samples were first polished mechanically and then finally on a vibrator. The samples were etched in a solution which had the following composition:

42 ml HF (conc.)

28 ml H_2SO_4 (conc.)

10 ml HNO_3 (conc.)

100 ml H_2O

The samples were etched by pouring the etching solution onto the polished sample surface. Etching was immediately interrupted when gas development occurred. With this method well reproducible, etching was achieved. Hardness measurements were made on polished and etched samples with a Leitz Durimet Small Hardness Tester under 1000 gr load. The reported hardness values are average values of approximately 10 indentations.

3.4 PHASE EXTRACTION METHOD

A number of methods are known, by which the chemical compositions of precipitates in columbium alloys can be investigated. With the Microprobe analyzer the metallic components of larger precipitates can be determined directly within the microstructure and thus the relationship is seen immediately between microstructure and precipitate. The non-metallic component of the precipitate, however, normally cannot be determined so that further analysis methods must be used. For instance, the lattice structure of the precipitate may be determined by x-ray or electron diffraction. The use of electron diffraction, however, is limited to such precipitates which are relatively fine and very thin. Another method of precipitate analysis is the mechanical or chemical isolation of precipitate particles from the surrounding matrix with subsequent lattice structure determination by x-ray structure analysis and composition determination by chemical analysis.

Microprobe analysis combined with x-ray structure analysis of chemically isolated particles was employed by Cuff (Reference 24) for the determination of precipitates in samples of molybdenum and columbium alloys. Begley and co-workers (Reference 17) used electron diffraction and x-ray structure analysis for precipitates in columbium alloys. Chang (Reference 16) employed x-ray structure analysis of electrolytically isolated precipitates in combination with x-ray fluorescence and chemical analysis in molybdenum and columbium alloys.

In the present investigation the precipitate particles were usually too small to give reliable results with the microprobe method. Therefore, the precipitate phases were extracted and x-ray structure analysis was performed with the intention to obtain information about the composition of the various precipitate phases by systematic variation of the sample condition. Where ever possible, chemical analysis of the extracted phases was performed.

For the isolation of the precipitate phases from heat treated samples a method was used at first which is described by Chang (Reference 16). The sample is electrolytically dissolved in a solution of methanol and 7 percent HCl. The results obtained by this method were not very satisfactory, since the residue contained generally a larger amount of matrix particles which make the analysis of x-ray patterns difficult and a chemical analysis of the residue meaningless. Efforts to improve this method were not successful.

Because of these difficulties a chemical extraction method was used which is described by Pochon et al. (Reference 1). The solution consists of 10 ml bromine, 90 ml methanol, and 10 grams tartaric acid. Approximately 35 ml of the solution was given into a test tube which contained the samples. The samples had a size of approximately 1/2 x 1/2 x 0.040 inches and were carefully ground, etched, and cleaned before extraction. Also with this method, difficulties were encountered particularly with samples of alloy D-31, since shortly after start of the reaction an apparently amorphous surface layer was formed, which slowed down the process. Fortunately, it was observed that in the immediate vicinity of a platinum wire, from which the sample was suspended, the reaction occurred relatively fast and without the formation of the surface film. In a number of tests it was found most beneficial to use a small basket of platinum mesh which contained the samples and which was suspended in the solution. This method was then used throughout the investigation. The samples were usually dissolved after approximately 24 hours. Subsequently the solution was centrifuged, decanted, and the isolated precipitate products were washed in methanol and dried in air.

Samples of the D-43 alloy usually dissolved faster than those of the D-31 alloy. In most cases no matrix contamination of the residue was found in the x-ray films. In order to determine if the precipitate phases were attacked by the solution, extracted precipitates from various heat treated samples were left in the solution for about three to four weeks. After this time neither a noticeable decrease in the amount of precipitates nor a change in the relative intensities of various precipitates from a single sample were observed. Since the precipitates in these alloys are mainly carbides, it is shown by these experiments that the carbides themselves are not attacked by the chemical reagents. Also, since the oxides are generally more corrosion resistant then carbides (Reference 25), one can conclude that at least these two types of precipitates are not essentially influenced by the chemical solution.

In the course of the investigation it was found that the limit of identification of precipitates by phase extraction and subsequent x-ray analysis corresponds with the limit of microscopic resolution, i. e., precipitates which have a size of less than 500 to 1000 Å were not detected in a direct way with these two methods. In several instances hardness measurements gave indications of the presence of such small precipitates, the identification of which could be only concluded from indirect evidence.

3.5 X-RAY ANALYSIS

Usually a few milligrams of precipitates were extracted from a single sample. This amount was too small to use a goniometer, therefore only Debye-Scherrer films were made. The dry powder was carefully mixed and filled into a 0.3 mm diameter Lindemann glass capillary. In many cases the amount of precipitate was sufficient for a second capillary for which the powder was then mixed with an internal standard (thoria or tungsten) in order to perform precision measurements. The x-ray powder patterns were made in a cylindrical Siemens camera with 114.6 mm diameter using type KK Kodak film. The non-symmetrical film arrangement was used to correct the film shrinkage. Most x-ray patterns were made with nickel-filtered copper radiation (λ = 1.54 Å).

Frequently the interference lines of the Debye-Scherrer patterns were somewhat diffuse which hampered the precise measurement of line position. Diffuse diffraction lines were mainly observed for precipitates which were formed during cooling from high temperatures or which had a very fine particle size. The larger, isothermally formed precipitates gave sharp diffraction patterns so that in many cases K separation could be observed in the back reflection region. Therefore, the more diffuse patterns seem to be caused by small particle size, concentration gradients, internal stresses, and lattice defects. For a comparison of the reported lattice parameters a maximum error of ±0.004 Å must be taken into consideration. In cases, where internal standards have been used, the error is decreased to about ±0.002 Å or less according to the condition of the sample.

For the evaluation of Debye-Scherrer patterns the measured lattice spacings d_o and the observed relative intensities I_o were compared with corresponding values of known crystal structures which presence was suspected according to the alloy composition. In some cases such a comparison led to a satisfactory identification of the compounds. Many precipitates in the investigated alloys have, however, NaCl-type structure which does not agree with the lattice parameters of pure compounds such as carbides, nitrides, and oxides. It is known that the pure carbides of the metals columbium, titanium, and zirconium form complete series of solid solutions (Reference 26). In the case of mixed carbides the composition can be determined from the measured lattice parameters of the precipitates. If, however, oxygen and nitrogen participate in the formation of precipitates, a decrease of the lattice parameter is usually encountered. In these cases determination of lattice parameters alone does not yield conclusive informaton on the composition, and one must resort to direct chemical analysis of the extracted precipitates for better identification.

SECTION IV

EXPERIMENTAL RESULTS AND DISCUSSION

4.1 COLUMBIUM ALLOY D-31 (Cb-10%Mo-10%Ti-0.1%C)

4.1.1 Precipitates in the As-Received Condition

The as-received condition is characterized by a series of cold-rolling and annealing processes (see Chapter 2.1). The intermediate heat treatments were done at 1200°C and the final annealing at 1100°C. The microstructure of the as-received condition, Figure 3a, shows almost complete recrystallization after the final annealing treatment. The precipitates in the as-received condition are not uniformly distributed in the microstructure but occur in patches and bands. The hardness of the as-received material, DPH = 208 kg/mm^2, corresponds to the hardness of the soft-annealed condition as can be seen from Figure 5.

The Debye-Scherrer pattern of extracted precipitates shows a number of interference lines, the d-values and intensities of which can be coordinated with a single lattice structure. The lattice is of the NaCl-type, the lattice parameter a = 4.322 ±0.001 Å. Lattice structure and parameter as well as the composition of the alloy may suggest that the precipitate is primarily TiC (a = 4.313 - 4.332 Å (Reference 27)). The chemical analysis of the precipitate*, however, gives the following values in weight-%:

Ti	47	±3%
Cb	45	±3%
Mo	2.5	±0.2%
C	8	±0.25%

* chemical analysis by Ledoux & Co.

The high columbium concentration of the precipitate is at first surprising. If the precipitate were a pure solid-solution carbide (Ti,Cb)C, one would expect a larger lattice parameter of at least 4.344 Å (Reference 26). It therefore must be assumed that oxygen and nitrogen participate in the precipitation of this phase which would decrease the lattice parameter. This assumption seems justified since according to the chemical analysis of the alloy D-31 (see Chapter 2.1) the weight ratio of oxygen + nitrogen to carbon is approximately 1/3. In Chapter 4.1.4 it will be shown further that by adding more oxygen to the alloy the lattice parameter of the precipitate is reduced even further. Therefore, it must be concluded that the precipitate in the as-received condition is a titanium-rich oxicarbonitride (Ti,Cb) (C, O, N). Since titanium and carbon are the main constituents of this precipitate it will be termed MC-phase. The subsequently described experimental results show that this precipitate is the equilibrium second phase in the alloy D-31.

4.1.2 Precipitates After Solution-Annealing

After annealing at higher temperatures the following changes occur in the microstructure and in the lattice structure of the precipitates. Coagulation of the MC-phase, a small amount of grain-boundary precipitates, and the beginning of grain growth can be observed in the microstructure after annealing 1hr/1400°C/FC. The Debye-Scherrer pattern shows a very weak line with a value of d = 2.25 Å in addition to the interference lines corresponding to the MC-phase. These changes are more prominent after annealing 1hr/1500°C/FC. Figure 3b shows the microstructure of such a sample. Beside the interference lines of the MC-phase, a number of additional weak lines can be observed in the x-ray pattern after this heat treatment. However, if the sample is quenched after annealing 1hr/1500°C/OQ, these additional lines and also the grain boundary precipitate are not observed; see Figure 3c. These results show that (a) the grain boundary precipitate occurs during cooling and that (b) the additional interference lines in the x-ray pattern seem to be caused by the grain boundary precipitate.

After annealing 1hr/1500°C/FC, the lattice parameter of the MC-phase had increased from 4.322 Å in the as-received condition to 4.342 Å which points towards a reduced stability of this phase. On the other hand the lattice parameter of the same phase after quenching from 1500°C was determined as a = 4.320 Å which is even slightly smaller than for the precipitate in the as-received condition. The latter phenomenon is explained by the lower vacuum in the quenching furnace (see Chapter 3.1) which causes an increase in the oxygen content of the sample and therefore a decrease of the lattice parameter of the MC-phase. This explanation is in agreement with the results of the internal oxidation experiments described in Chapter 4.1.4.

Figure 3d shows the microstructure after annealing 1hr/1600°C/FC. The most striking differences between this and the previous microstructures are the marked grain growth, the needle shape and more uniform distribution of the precipitates, and the grain boundary precipitate film. If the sample is quenched in an oil bath after annealing 1hr/1600°C/OQ, the microstructure as shown in Figure 3e is essentially a single phase structure.

These annealing experiments show clearly that the MC-phase has dissolved at 1600°C. The needle-like precipitates and the grain-boundary precipitate must have formed during fast radiation cooling (FC). Repeated annealing of the oil-quenched sample at 1600°C with subsequent radiation cooling gave again a needle-like structure which corresponds to Figure 3d. It is therefore shown that by quenching from 1600°C the formation of observable precipitation can be suppressed in this alloy.

For radiation cooled samples (FC) the microstructures after annealing at 1600° and 1700°C are quite similar (compare Figures 3d and 3f), although the amount of precipitate has slightly decreased after annealing at 1700°C. After quenching from 1700°C in oil, however, precipitates

are observed again, as is shown by Figure 3g. The precipitate-free zones along the grain boundaries are typical for heterogeneous precipitation from supersaturated solid solution. The fact that precipitation is not suppressed during quenching from 1700°C is attributed to the additional amount of heat which must be dissipated and which gives a lower quenching rate. This observation illustrates the extreme rate of precipitation in columbium alloys.

The average grain size after one hour annealing at various temperatures is plotted in Figure 4. As was mentioned earlier, grain growth starts at 1400°C. A sudden increase of grain size occurs during annealing between 1500° and 1600°C. This behaviour is noteworthy, since grain growth occurs in the same temperature region in which increased solutioning of the MC-phase was observed. The temperature of sudden grain growth coincides with the temperature region of complete solid solution.

The hardness of the alloy D-31 after one-hour anneals at various temperatures is plotted in Figure 5. Recovery from cold work starts at 900°C. Alloy D-31 has reached the lowest hardness after annealing in the temperature region between 1100° and 1300°C. Above this temperature region the hardness increases continuously until at approximately 1600° to 1700°C maximum hardness is obtained. It is noted again that the hardness increase occurs in the temperature region of increased solutioning of the MC-phase. Higher hardness values are obtained after quenching than after fast radiation cooling (FC). The precipitation-free sample, Figure 3e, shows the highest hardness value of 313 kg/mm^2. After quenching from 1700°C the hardness is decreased to 283 kg/mm^2. Observation showed that as the samples increased in hardness they became more brittle at room temperature.

The results of the annealing tests for the alloy D-31 are summarized as follows: At 1400°C strong coagulation as well as solutioning of the MC-phase occurs. With beginning solutioning grain growth, hardness increase, and room temperature embrittlement are observed simultaneously. The minimum temperature of complete solid solution for the alloy D-31 is approximately 1580° ±30°C. After solution annealing in conventional radiation-cooled vacuum furnaces precipitation cannot be prevented during cooling. These non-equilibrium precipitates form as a film at the grain boundaries as well as thin platelets in the grain interior.

The Introduction states that previous investigators have observed disappearance of precipitates in the microstructure of Cb-alloys after annealing at temperatures approaching the melting point, which was interpreted as a solid solutioning effect. Since this interpretation disagrees with the present findings, it is suspected that the disappearance of precipitates is due to a decarburization or, generally, degassing at high temperatures. This suspicion is verified by the chemical analysis of two D-31 samples, each annealed for one hour at 1700°C in one of the two high-temperature annealing furnaces (see Chapter 3.1). The results are compared in Table I together with the analysis of the as-received sample. While the nitrogen content is nearly unaffected, appreciable carbon loss and an increase of oxygen concentration occurred. It is also seen that the lower vacuum of the quenching furnace favours decarburization. When a sample was annealed for 18 hours at 1700°C/FC, no precipitates were observed in the microstructure, its hardness reached a low value of 230 kg/mm^2, and it was quite ductile at room temperature.

The x-ray analysis of precipitates extracted from solution-annealed samples of alloy D-31 (i.e. precipitates which have formed during cooling) yielded a number of interference lines which belong to a precipitate with a yet unknown lattice structure. That these interference lines were caused by a single precipitate phase was ascertained by suitable variation of the heat treatment so that a change of intensities of the lines against those of other precipitates was achieved. Further-more, the same precipitate was found in the columbium alloy D-43 (see Chapter 4.2) and in this alloy the precipitate was separated as a single phase after some special treatments (see Chapter 4.2.4). This precipitate is essentially a columbium carbide which may under some conditions dissolve other alloying elements like molybdenum, titanium,

tungsten, zirconium, and oxygen. This carbide will be designated as ϵ-carbide, In the microstructure it occurs in form of larger or smaller platelets and as a grain boundary precipitate.

Increased solutioning of the MC-phase occurs after annealing at 1400° and 1500° C and a precipitate phase forms at the grain boundaries during cooling. The interference lines in the x-ray patterns which were apparently caused by the grain boundary precipitate are identical with those of the ϵ-phase. This shows that the ϵ-phase can precipitate during cooling in the temperature region below 1400°C.

Beside the ϵ-phase a second strong precipitate was determined in the D-31 alloy after solution annealing. This precipitate has a lattice structure of the NaCl-type and a lattice parameter which, depending on the previous heat treatment, has a value around a = 4.39 Å. An exact analysis of the composition of this precipitate was not possible, since both this and the ϵ-carbide occurred always simultaneously. A comparison of the lattice parameter of this FCC-phase with that of the cubic CbC (a = 4.431 — 4.470 Å (Reference 28)) suggests that CbC plays a major role in this precipitate phase. A decrease of the lattice parameter to a = 4.39 Å and less can be caused by the substitution of Cb by Ti and Mo and also by the substitution of C by O. Oxygen may play a major role in the precipitation of this phase, since the diffusion rate of oxygen is comparable to that of carbon and since oxygen is present in considerable amounts as can be taken from Table 1. On the basis of the determined lattice parameter this precipitate is assumed to be a columbium-rich oxicarbide (Cb,Ti,Mo) (C,O).

Beside relatively strong interference lines of the ϵ-carbide and of the cubic oxicarbide usually a few additional but very weak lines were observed which may have been caused by traces of hexagonal Cb_2C and cubic CbC. The CbC-phase was more prominent after quenching than after slower radiation cooling. Because of the relatively weak and diffuse diffraction pattern it was not possible to determine precisely the lattice parameter of these precipitates so that no further information was gained about their exact composition. The presence of these weak precipitate phases may be due to the heterogeneity of the precipitation processes during cooling. A summary of the precipitate phases which were identified in the columbium alloy D-31 after various heat treatments is given in Table II.

It is now necessary to establish a relationship between the precipitates observed metallographically and by x-ray methods. For solution annealed samples the Debye-Scherrer pattern gave essentially two different precipitates, the ϵ-phase and the cubic oxicarbide. In the microstructures of Figures 3d and 3f, however, only one type of precipitate can be seen. Electron micrographs of surface replica were taken to increase the resolution of the optical micrographs. Figures 6a to 6c show the microstructures of samples which were, respectively, quenched, fast-cooled, and slow-cooled after annealing for one hour at 1700°C. These microstructures also suggest only one type of precipitate which occurs in the form of thin platelets or needles. By decreasing the cooling rate the size of these precipitates increases. It must therefore be concluded that both the ϵ-carbide and the cubic oxicarbide show the same precipitate form in the microstructure. Because of the large grain size after solution annealing the amount of grain boundary precipitate is too small to account alone for the high intensity of one of the two major phases in the Debye-Scherrer pattern.

It may be stated in summary, that after solution annealing alloy D-31 precipitates occur upon cooling which are columbium-rich carbides or oxicarbides. As will be more clearly shown by the investigation of precipitates in the columbium alloy D-43 in Chapter 4.2, the formation of the ϵ-phase depends on the degree of under-cooling and on the carbon concentration. This behaviour can also be gathered from the results summarized in Table II. Based on these results and those which are reported in Chapter 4.2 it must be concluded that the cubic oxicarbide precipitates in an upper temperature region and the ϵ-carbide in a lower temperature region during the cooling process.

4.1.3 Aging Experiments

This chapter describes results of a series of tests which were performed for the purpose of obtaining information about the precipitation phenomenon which caused the increased hardness of solution annealed samples, see Figure 5. Chapter 4.1.2 shows that columbium-rich carbides precipitate during cooling from high temperatures. For the relatively large size of these carbides it is improbable that the hardness increase should be caused by them. Another purpose of this test series was to determine the possibility of age-hardening in the alloy.

For the aging tests, sheet samples of alloy D-31 were solution annealed for one hour at 1700°C. One portion of the samples was quenched in oil (OQ), the other portion was radiation cooled (FC). The solution annealed samples were subsequently aged for one hour at temperatures between 250° and 1300°C.

The hardness data of the aged samples are plotted in Figure 7. Within the scatter of the hardness values for fast-cooled samples no tendencies towards age-hardening can be observed. Above 900°C the hardness decreases rapidly and reaches a minimum at temperatures between 1200° and 1300°C. However, for the quenched samples a hardness maximum is clearly indicated at 450°C. Above 450°C the hardness decreases first and then remains constant within the scatter of the values up to about 950°C. Aging at higher temperatures results in a parallel hardness decrease as for fast-cooled samples and the hardness minimum is also reached between 1200° and 1300°C. Due to the scatter of the hardness values it cannot be stated with certainty whether a second age-hardening peak exists in the temperature region between 800° and 1000°C.

Typical changes of microstructure during aging are illustrated by comparing Figure 3f with Figure 8. After one hour aging at 1200° and 1300°C the originally precipitate-free regions between the needle-like precipitates and the immediate vicinity of these needle-like precipitates now contain clearly a fine, dispersed precipitation. The precipitate-free regions in the neighborhood of the needle-like precipitates and the grain boundaries are further worthy of notice. These microstructural changes can be observed at first after annealing in the temperature region between 1000° and 1100°C in solution annealed and fast-cooled samples, i.e., in the temperature region of the rapid hardness decrease.

Analysis of x-ray patterns of extracted precipitates gives some explanation about the phase changes which occur during aging. These results are also summarized in Table II. During aging for one hour at 1200°C the ϵ -carbide phase has almost disappeared. Simultaneously another cubic phase has appeared with a lattice parameter of approximately a = 4.34 Å. The columbium-rich oxicarbide phase with a lattice parameter of a = 4.39 Å is, however, still present. The new cubic phase may be identified as the titanium-rich MC-phase, since after aging for 16 hours at 1200°C only this phase is present which, therefore, is the stable precipitate phase in this temperature region. The observed broadening of the interference lines for the MC-phase gives a further indication that this phase exists in very fine particle size and therefore corresponds to the fine precipitation which is observed in Figure 8.

These results show that the ϵ -phase is less stable in the temperature region around 1200°C than the cubic, columbium-rich oxicarbide which dissolves only after prolonged aging at these temperatures.

An explanation for the age-hardening peak at 450°C of oil-quenched samples cannot be given with certainty. The microstructure as well as the x-ray results do not indicate any changes which could be related with this anomaly. A more precise analysis of the Debye-Scherrer patterns of these quenched and aged samples was not possible because of some small variations in the amounts of the precipitate phases from sample to sample. Such variation in the

precipitate phases may have been caused by minute differences of the quenching conditions within the samples since, as pointed out earlier, the quenching rate is quite critical. An analogous but more pronounced age-hardening peak was also found in quenched samples of the alloy D-43, as will be shown in Chapter 4.2.3. The investigation of microstructure and precipitate phases in the alloy D-43 suggests that the age-hardening peak is related to precipitation or transformation of one of the columbium carbides.

The further observation in Figure 8, i.e., the precipitate-free zones in the neighborhood of the needle-like precipitates and the grain boundaries, deserves further discussion. The fine, dispersed MC-precipitate in the regions between the needle-like columbium carbides suggests a relatively homogeneous nucleation. If this precipitation of the MC-phase is exclusively caused by dissolution of the columbium carbides, the precipitate-free zones in the neighborhood of the coarse columbium carbides cannot be explained. One would rather expect that the MC-precipitate occurs at or near the dissolving columbium carbides, since the carbon content is many times overcompensated by the titanium content. From the existence of the precipitation-free zones one has to conclude that nucleation and growth of the fine, homogeneously distributed MC-phase occurred at the same time as did the precipitation of the Cb-carbides, i.e., during cooling from the temperature region of solid solution. After solution annealing, the titanium-rich MC-phase must be present in a state, in which it cannot be identified by the methods of phase extraction or by electron microscopy of surface replica. It is therefore not surprising that in this state the MC-phase has a strong hardening effect and causes the hardness of the solution annealed samples (see Chapter 4.1.2 and Figure 5). As soon as the MC-precipitates can be identified in the microstructure by aging in the temperature region between 1000° and 1300°C, considerable coagulation has already occurred causing a decrease of hardness.

This interpretation blames the high hardness of the solution annealed D-31 samples on the titanium content. Since nucleation and growth kinetics of the non-isothermally formed MC-phase depend on the titanium concentration of the alloy, a smaller titanium content should result in lower hardness after solution annealing.

A small alloy button of the composition Cb-10%Mo-1%Ti-0.1%C was prepared*) and hardness measurements were conducted on sections of this button after one-hour anneals at various temperatures between 1200° and 1900°C. Figure 9 shows the measured hardness values along with those of the alloy D-31. The hardness of the experimental alloy is equal to the hardness of the soft-annealed alloy D-31 and remains approximately constant after various heat treatments.

With this supporting evidence the results of this test series may be summarized briefly as follows. The high titanium concentration of alloy D-31 permits precipitation of the stable MC-phase simultaneously with the formation of unstable columbium carbides during rapid cooling from the temperature region of solid solution. The non-isothermally formed MC-phase is stable up to approximately 900°C and coagulates upon aging at higher temperatures. The hardness increase after solution annealing is caused by this MC-phase. The unstable columbium carbides were observed to dissolve in favor of the formation of isothermal MC-phase at 1200° and 1300°C. Of the unstable columbium carbides the ϵ-carbide is less "stable" than the cubic oxicarbide. The one-hour aging tests did not give any certain indication of age-hardening effects from the precipitation of isothermal MC-phase. An age-hardening phenomenon, however, was observed for oil-quenched samples in the temperature range around 450°C. The reason for the age-hardening peak was not ascertained but may involve the precipitation or transformation of an unstable columbium-rich carbide.

*)The alloy button was melted in a water-cooled copper crucible under argon at the University of Dayton, Research Institute. Carbon was added in form of CbC.

4.1.4 Effect of Oxygen on Carbide Precipitation

The previously described results do not give any indication for the presence of metallic oxides in alloy D-31, although the oxygen content was strongly increased during some annealing treatments (see Table I). On the other hand, for the interpretation of the phase analysis the assumption was frequently made that oxygen participated in the formation of carbides. The monocarbides CbC and TiC form a complete series of solid solutions (Reference 26). That the same solubility exists also for oxicarbides cannot be assumed with certainty since the columbium oxide CbO is known to have an ordered defect structure (Reference 29). It was therefore necessary to obtain some further information in proof of the previous assumptions.

For this purpose experiments were conducted in the following way: A sample of the as-received alloy D-31 was charged with oxygen at 900°C to a level of 0.08 percent. After various heat treatments the precipitates were extracted from the sample and analysed by the x-ray powder method. The results are summarized in Table III.

After annealing for 16 hours at 1200°C, two precipitates with NaCl-type lattice structure were determined. The minor phase had a lattice parameter equal to that of the precipitate phase in the as-received condition (a = 4.322 Å) and is therefore identical with (Ti, Cb) (C,O,N). The major precipitate phase with a lattice parameter of a = 4.292 Å must be caused by the added oxygen. However, this precipitate cannot be a pure oxide since the lattice parameter is larger than that of both metallic oxides TiO (a = 4.177 Å) and CbO (a = 4.21 Å). It is assumed that this major precipitate phase is an oxicarbide of the metals columbium and titanium. To determine whether phase equilibrium was achieved after 16 hours at 1200°C, the sample was annealed for additional 10 hours at 1300°C. After this heat treatment, only one precipitate phase was identified. The lattice parameter of this single phase is a = 4.300 Å which is smaller than that of the precipitate in the as-received condition and larger than the lattice parameter of the second strong phase after the previous annealing treatment at 1200°C. These results show conclusively that the lattice parameter of the stable MC-precipitate in the alloy D-31 is decreased by the higher oxygen content. It is evident that oxygen is soluble in the Ti-rich monocarbide to a considerable extent. Since no chemical analysis was made, it cannot be stated whether the ratio of titanium to columbium in the MC-phase was changed by the higher oxygen concentration.

An important consequence of these test results is that no metallic oxide is formed in the alloy D-31 under the given circumstances but only an oxicarbide. This means that the oxicarbide is thermodynamically more stable than the carbide and oxide, respectively. Chapter 4.2.4 will show that this is not the case in the zirconium-containing alloy D-43.

A second part of the oxygen-rich sample was solution annealed for one hour at 1700°C and fast cooled in order to determine the effect of oxygen on the precipitates which form during cooling. Table III shows that after solution annealing the oxygen-rich sample, the ϵ-carbide was the major precipitate phase. The lattice parameter of the cubic oxicarbide phase of a = 4.39 Å was somewhat lower than that of the same phase in the oxygen-low sample, which may be interpreted in terms of a larger O/C ratio. The smaller volume ratio of oxicarbide to ϵ-phase in the oxygen-rich sample than in the oxygen-low sample can be explained on the basis that the cubic oxicarbide is formed during cooling in a higher temperature region than the ϵ-phase and that a stronger decarburization occurred during solution annealing of the oxygen-rich sample. Chemical analysis of a sample with initially 0.052 percent oxygen showed a carbon concentration of only 0.045 percent and an oxygen concentration of 0.028 percent after solution annealing for 1hr/1700°C/FC. Compared to the as-received sample (see Table I) this constitutes a further loss of carbon by 0.02 percent.

Chapter 4.1.3 shows that the titanium-rich MC-phase precipitates during cooling after solution annealing which causes a large hardness increase. Since the MC-phase in this case cannot be detected by metallographic nor by phase extraction methods, the results mentioned before do not give any information about the role of oxygen in this phase. The data summarized in Table IV also do not indicate a simple dependence of hardness after solution annealing on the original oxygen content of D-31 samples, although the hardness values of oxygen-rich samples are generally higher than of as-received and solution annealed samples.

4.2 COLUMBIUM ALLOY D-43 (Cb-10%W-1%Zr-0.1%C)

4.2.1 Precipitates in the As-Received Condition

As is shown by the processing history, Chapter 2.2, the alloy sheet D-43 was annealed for 10 minutes at 1650°C before the last cold rolling reduction and finally annealed for 1hr at 1425°C in vacuum. The microstructure, Figure 10a, indicates almost complete recrystallization. Numerous precipitates are observed at grain boundaries and in the grain interior; the majority of particles appear to be globular, others have needle or platelet form.

The results of x-ray structure analysis of precipitates in the as-received condition are summarized in Table V. There appear to be three different kinds of precipitates; the major phase has NaCl-type lattice with a = 4.51 Å; from the two medium strong phases one has also a cubic lattice with a = 4.60 Å, the other is hexagonal. The Debye-Scherrer film shows a continuous darkening between two diffracted lines corresponding to identical index planes of the two cubic phases. This indicates the existence of numerous precipitates with NaCl-type lattice and lattice parameters between 4.60 and 4.51 Å. It must be assumed that one of the cubic precipitates is not in equilibrium with the other cubic phase and has most likely formed during one of the previous heat treatments. Further evidence shows that the two cubic phases form a continuous series of solid solutions with each other.

Because of the number of precipitate phases, a direct chemical analysis of the precipitates is not meaningful and it is only possible to estimate the composition of the three precipitate phases by comparison of the lattice structures and parameters. The hexagonal phase is most certainly identified as Cb_2C, since the x-ray diffraction patterns of both compounds are almost identical. The small deviation of cell size may be caused by the solution of other alloying elements like tungsten and zirconium.

Since both the oxygen and nitrogen content of alloy D-43 are very low (see Chapter 2.2), it is safe to assume the two cubic phases to be mixed carbides of essentially columbium and zirconium. Chang (Reference 16) found a precipitate phase with a = 4.60 Å in the columbium alloy F-48, which was zirconium-rich and contained columbium. Assuming that only traces of oxygen and nitrogen are present, the ratio of zirconium to columbium can be calculated from the data of Norton and Mowry (Reference 30) to be at least 2/1 for the carbide with a = 4.60 Å. This ratio is in very good agreement with results of chemical analysis reported by Chang. Chapter 4.2.4 will show that in the presence of oxygen in the alloy D-43 the Zr-rich MC-phase is not stable, which means that it has only a low solubility of oxygen. It seems justifiable, therefore, to identify this cubic phase (with a = 4.60 Å) as zirconium-rich (Zr,Cb)C.

In analogy a conclusion is drawn that the major cubic precipitate with a = 4.51 Å is most probably a columbium-rich monocarbide (Cb,Zr)C. The above cited data of Norton and Mowry give a ratio of Zr/Cb = 1/3 for a lattice parameter of a = 4.51 Å. The results reported in Chapters 4.2.2 and 4.2.3 indicate a dependence of the Zr/Cb ratio on annealing temperature; the ratio decreases with increasing annealing temperature.

4.2.2 Solution Annealing

This chapter describes the phase changes occurring in alloy D-43 during annealing treatments at temperatures at and above 1400°C. It will become evident that the cubic MC-phase is the stable precipitate in alloy D-43 (as it is for alloy D-31) although the concentration of zirconium is only one atomic percent (against 17 at.-% Ti in alloy D-31). The low zirconium content of alloy D-43 has a bearing on the precipitates occurring after solutioning of the MC-phase, but it will become apparent that the general precipitation behaviour of alloy D-43 is very similar to that of alloy D-31 with regard to carbide phases.

First, it is necessary to establish which of the precipitates observed in the as-received condition is the stable phase. Further annealing at 1400°C, the temperature of the final annealing treatment during processing (see Chapter 2.2) results in a steady increase of the zirconium-rich (Zr,Cb)C, which seems to grow predominantly on the expense of the hexagonal Cb_2C phase (see Table V). Phase equilibrium is not achieved after additional 16 hours at 1400°C, but longer annealing at 1400°C is not advisable since the x-ray powder data show the formation of zirconium oxide after the 16 hour anneal. The formation of ZrO_2 is caused by increased contamination and disturbs the phase equilibrium. Nevertheless, the annealing experiments at 1400°C indicate that the zirconium-rich monocarbide (Zr,Cb)C with a lattice parameter of a = 4.60 Å is the stable equilibrium precipitate phase. Table V shows that the zirconium-rich MC-phase dissolves increasingly upon annealing at temperatures above 1400°C. After annealing 1hr/1600°C/FC the (Zr,Cb)C is present only in weak amounts and disappears completely after annealing 1hr/1650°C/OQ.

The columbium-rich carbide (Cb,Zr)C, however, does not appear to be affected by these annealing treatments. Since CbC and ZrC form a complete series of solid solutions and since the zirconium-rich (Zr,Cb)C is stable at 1400°C and dissolves above this temperature, one is led to conclude that the columbium-rich (Cb,Zr)C has formed during the 1650°C annealing treatment in the fabrication process (see Chapter 2.2). This implies that the ratio Zr/Cb of the monocarbide is temperature dependent, a phenomenon which is more clearly shown by aging experiments in Chapter 4.2.3.

With increasing dissolution of the MC-phase the Debye-Scherrer films show growing amounts of Cb_2C and ϵ-carbide. When the MC-phase dissolves completely at temperatures above 1650°C, only Cb_2C and ϵ-carbide are observed. During investigations of the columbium alloy F-48 Chang (Reference 16) made similar observations and assumed that the Cb_2C was stable between 1650° 2000°C.

Numerous attempts were made to quench samples of alloy D-43 after annealing at high temperatures in an oil bath to prevent the formation of precipitation during cooling. This method, which proved helpful in determining the temperature region of solid solution for alloy D-31, failed to give similar direct evidence for alloy D-43. However, a number of observations yields enough evidence to conclude that Cb_2C and ϵ-carbide are not equilibrium phases in alloy D-43 but have formed during cooling from high temperatures.

If the columbium carbides have formed during cooling, large differences in cooling rate would certainly influence the type and amount of precipitates. In addition to quenching in oil three slower cooling rates were employed after annealing at 1900°C which are plotted in Figure 2. The phase analysis from Debye-Scherrer patterns of precipitates from differently cooled samples is summarized in Table V. With regard to Cb_2C and ϵ-carbide it is seen that the relative amount of Cb_2C increases with a decreasing cooling rate, the ϵ-carbide behaving inversely. The only regular interpretation of this behaviour is that both carbides, ϵ and Cb_2C, have precipitated during cooling and that the Cb_2C precipitates in a somewhat higher temperature region than the ϵ-carbide.

For one-hour annealing treatments at 1800°, 1900°, and 2000°C with identical cooling rates (FC) the data of Table V show a slight decrease of the relative amount of Cb_2C with increasing annealing temperature. This diminution of Cb_2C phase points toward a change in chemical composition unless the above arguments are incorrect. From chemical analysis of solution annealed samples (see Table VI) it is evident that decarburization occurs at high temperatures in conventional vacuum annealing furnaces, as was shown earlier for alloy D-31. The low oxygen content after solution annealing is surprising, since analogous experiments with alloy D-31 resulted in a rather large increase of oxygen concentration (compare Table I).

Changes of microstructure after annealing alloy D-43 at various high temperatures are illustrated in Figure 10. A comparison of Figures 10b and 10a and the respective data in Table V suggests that the increased platelet-like precipitate phase after annealing 1hr/1600°C/FC is identical with Cb_2C. After 1hr/1700°C/FC only platelet-like precipitates appear in the microstructure, see Figure 10c. Except for the large grain growth and increased platelet size no essential microstructural changes can be observed after annealing at still higher temperatures. The platelet form of the precipitate phase is shown by the overetched microstructure of Figure 10d. Figure 11 illustrates the effect of cooling rate on the microstructure after annealing at 1900°C. There is no great difference between fast (FC) and slow-cooled (SC) samples, Figures 11a and b; but the very slow-cooled (VSC) sample, Figure 11c, shows quite a different distribution and size of precipitates. A close observation also reveals an apparent increase of thickness of the grain boundary precipitate with decreasing cooling rate. After oil-quenching from 1900°C an additional fine, dispersed precipitate can be observed in the spaces between the platelets. The precipitate-free surrounding of the coarse particles suggests that the fine dispersion has formed in the same or in a somewhat lower temperature region than the coarse platelets. Chapter 4.2.3 will show that the dispersed phase has a much lower thermal stability than the coarse one. The data in Table V shows that a small amount of CbC was determined beside Cb_2C and ϵ-carbide only after quenching from the temperature range of solid solution. Therefore, the CbC phase appears to be identical with the fine dispersion in Figure 11d.

Figure 12 is a plot of grain size versus annealing temperature for one-hour anneals. The sudden grain growth between 1600° and 1700°C is noteworthy, because this temperature coincides with that for solution of the MC-phase. Referring again to Figures 10 and 11, another point of interest is the obvious orientation relationship between grain matrix and precipitate. The platelet-like precipitate phase, therefore, can have formed only at the end of grain growth. These phenomena, i.e. grain growth, precipitate-matrix orientation relationship, and also the results of x-ray phase analysis, give sufficient evidence that complete solid solution is achieved in alloy D-43 at temperatures at and above 1700°C. The large platelet size of Cb_2C and ϵ-carbide in fast cooled and quenched samples illustrates impressively the rate of carbide precipitation in this alloy.

Hardness values of alloy D-43 are plotted in Figure 13 for various annealing treatments. Recovery from cold work is characterized by the hardness decrease after one-hour anneals between 1000° and 1300°C. A hardness increase is not observed after solution annealing alloy D-43, which is in contrast to alloy D-31 but confirms the effect of low concentrations of MC-phase-forming elements like Ti or Zr (see Chapters 4.1.2 and 4.1.3). The platelet-like precipitates have no essential influence on the hardness of alloy D-43.

4.2.3 Aging Reactions.

The high rate of precipitation of Cb_2C, ϵ-carbide, and CbC seems to make a carbon supersaturation in alloy D-43 impossible with the experimental procedures used and generally very difficult for large samples. The columbium carbides, on the other hand, are not

stable with respect to the zirconium-rich MC-phase, so that aging reactions are expected to occur upon heating such samples below the solid-solution temperature range. To study the aging reactions samples were solution annealed 1hr/1900°C. One batch of samples was oil-quenched (OQ), the other was fast cooled (FC), (see Figure 2).

The average hardness values after one-hour aging at temperatures between 250° and 1300°C are plotted in Figure 14. Quenched samples show a pronounced age-hardening peak at 400°C. Since fast-cooled samples do not show this anomaly, the hardness peak cannot be caused by contamination or internal oxidation during aging.*) Above 700°C the hardness curves for both, fast-cooled and quenched samples maintain a relatively constant level. It is assumed that the hardness data above 800°C show some influence of contamination during aging. A pronounced age-hardening peak does not occur in this temperature region.

The experimental results do not give conclusive evidence about the mechanism responsible for the age-hardening peak at 400°C. After solution annealing and quenching the microstructure showed a fine, dispersed precipitate (Figure 11d) which was identified as CbC and does not occur in solution annealed, fast-cooled samples (Figure 11a). This dispersion has coarsened slightly during aging at 624°C, as is shown by Figure 15 a. The CbC-precipitate phase, however, cannot be detected after this aging treatment in x-ray powder patterns. The dispersion in Figure 15a, therefore, is no longer CbC, but most likely ϵ-carbide. Aging of quenched samples at temperatures above 800°C results in an almost complete disappearance of the dispersed phase, as is illustrated by Figure 15b. In summary, it seems to be safe to attribute the one-hour age-hardening peak at 400°C of solution annealed and quenched samples to a precipitation or transformation reaction of columbium carbides, although the precise mechanism eludes further analysis.

Precipitation of stable, zirconium-rich MC-phase was first detected after aging at temperatures above 1100°C. The MC-phase can be observed easily in the microstructure due to its comparatively small size and apparently different morphology (see Figure 16). An orientation dependence of etching response is evident from Figure 16b. Based on metallographic observation the time-temperature dependence of MC-phase precipitation was determined for both batches of samples (i.e. quenched and fast-cooled). The results are plotted in Figures 17a and 17b. The boundary curves represent approximately 5 percent and 95 percent MC-phase precipitation. A comparison of both figures reveals a retardation of MC-precipitation in fast-cooled samples relative to quenched samples. The rate of MC-precipitation is fastest at approximately 1400°C and seems to decrease at higher temperatures giving the boundary limits a C-profile. X-ray diffraction analysis of extracted precipitates supported the metallographic observations that the MC-precipitation is retarded above 1400°C.

Roche (Reference 31) found reduced tensile ductility in D-43 alloy samples, which were solution annealed and slowly cooled, corresponding to cooling curve SC in Figure 2. The ductility was improved by aging these samples at temperatures between 980° and 1425°C. The time-temperature data for the beginning of ductility improvement from Roche's work are plotted as dotted lines in Figures 17a and b, and coincide approximately with the beginning of MC-phase precipitation. This coincidence suggests strongly that the observed restoration of tensile ductility is caused by dissolution of Cb_2C and ϵ-carbide. Both columbium carbides were previously shown (see Chapter 4.2.2) to precipitate at grain boundaries as well as in the grain interior during cooling after solution annealing and seem to be responsible for the embrittlement observed by Roche. The grain boundary film, which may be the very source of embrittlement, is seen in Figure 16b to break up during aging.

*) Relatively simple dilatometric measurements have also indicated microstructural instability of EB-melted C-containing Cb-alloys in the temperature region between 250° and 500°C (Reference 34).

An interesting phase transformation occurs during aging, which is not detected by metallographic observations. The lattice structure of the ϵ -carbide was observed to undergo changes during aging at temperatures above 800°C. Since the lattice structure is not known, these changes cannot be described in physical details but only by comparison of the diffraction data, which are summarized in Table VII. The last column of Table VII represents the diffraction data for Cb_2C from the work of Elliott (Reference 2). Following the observed d-values of individual reflections during the various stages of aging, it becomes apparent that a number of d-values of the transformed ϵ -carbide corresponds with those of Cb_2C. Other lattice spacings of Cb_2C, notably those for which the 1-index is an odd integer, e.g. (10.1), (10.3), (10.5), (20.3), (21.1), and (21.3), seem to be split up in the transformed ϵ -carbide, which is indicated by the symbols between the last two columns. It is assumed that the ϵ -phase is being transformed upon aging into Cb_2C. The transformation cannot be followed to completion, since the columbium carbides dissolve in favor of MC-precipitation.

A characteristic behavior of the MC-phase in alloy D-43 can be observed in the x-ray analysis of precipitates in aged samples. The lattice parameter of the cubic monocarbide (Zr,Cb)C depends upon the aging temperature, which is shown by the data in Table VIII and was already pointed out in the discussion of Chapters 4.2.1 and 4.2.2. The decreasing lattice parameter with increasing aging temperature is not caused by oxygen solution (as was found for the titanium-rich MC-phase of alloy D-31), a statement which will be justified in Chapter 4.2.4. The only explanation of this phenomenon is the substitution of zirconium by columbium. Assuming that tungsten does not take part in this process, the ratio of Zr/Cb can be approximately calculated from the observed lattice parameters using the data of Norton and Mowry (Reference 30). The Zr/Cb values are maximum values, since the data of Norton and Mowry refer to almost stoichiometric compositions of the mixed carbide (Zr,Cb)C, and stoichiometry will most probably not be achieved for precipitates in columbium alloys. The dependence of the Zr/Cb ratio on temperature above 1200°C is an indication of increased instability of the MC-precipitate, so that precipitation-hardening seems to be little effective above 1200°C.

4.2.4 Internal Oxidation

Metallic oxide phases are not present in columbium alloy D-31 due to the large solubility of the titanium-rich MC-phase for oxygen. After solution annealing columbium alloy F-48 Chang (Reference 16) found monoclinic ZrO_2 precipitation which seemed to dissolve upon aging at 1370°C in favor of (Zr,Cb)C formation. No explanation was given for the state of oxygen in alloy F-48 after dissolution of ZrO_2. Alloy D-43 has a composition similar to alloy F-48 but smaller concentrations of oxygen and nitrogen. An indication of ZrO_2 formation was previously observed upon prolonged heating alloy D-43 at 1400°C, (see Chapter 4.2.2) which apparently resulted from contamination during annealing. The discrepancy of experimental results makes it desirable to study the behavior of oxygen in alloy D-43 during heat treatments. For this purpose samples of as-received alloy D-43 were charged with oxygen at 900°C, heat treated at various times and temperatures, and dissolved in the bromine-methanol-tartaric-acid solution for the determination of precipitate phases. The results are summarized in Table IX.

A D-43 sample with 0.14 percent oxygen was annealed for two hours at 1000°C. Compared to the as-received condition the following phase changes are observed (see Table IX). The columbium-rich MC-phase with a = 4.51 Å is still present in the same amount, but the zirconium-rich MC-phase with a = 4.60 Å has completely disappeared. The amount of Cb_2C has grown and, in addition, ZrO_2 precipitation was detected.

Another sample with 0.026 percent was annealed for 16 hrs at 1400°C. The phase determination results for this sample may be compared to those for a non-contaminated sample

with the same heat treatment (see Table V). The amount of the zirconium-rich MC-phase with a = 4.60 Å remained unaltered, yet the columbium-rich modification (Cb,Zr)C has disappeared. The amount of Cb_2C precipitate is slightly increased and ZrO_2 has formed in addition.

These results indicate that the MC-phase in alloy D-43 does not dissolve any measurable amounts of oxygen, since the lattice parameters did not change during the annealing treatments. The increased Cb_2C precipitation in both samples was made possible by the dissolution of one of the two monocarbide phases. The ZrO_2 phase has accordingly formed on the expense of the monocarbides. Therefore it is evident that the ZrO_2 phase is more stable than the mixed monocarbides in the temperature region between 1000° and 1400°C. At 1400°C the columbium-rich monocarbide (Cb,Zr)C was previously found to transform slowly into (Zr,Cb)C (see Chapter 4.2.2). In the presence of oxygen the rate of dissolution of (Cb,Zr)C becomes considerably faster. It is believed that the high affinity of zirconium for oxygen is responsible also for the preferred dissolution of the zirconium-rich (Zr,Cb)C at 1000°C, even though it is slightly more stable than the columbium-rich (Cb,Zr)C.

Annealing of oxygen-rich samples at 1900°C/FC does not produce any indication for ZrO_2 precipitation (see Table IX), but oxygen appears to decrease the amount of Cb_2C relative to the ϵ-carbide. To guard against erroneous interpretation, the carbon and oxygen contents were analyzed* in a sample which was charged with oxygen up to a level of 0.057 percent prior to annealing for 1hr/1900°C/FC:

carbon	0.0328%
oxygen	0.0016%.

Compared to the analysis of an as-received D-43 sample with the same heat treatment (see Table VI, Furnace A) a total loss of the additional oxygen occurred together with a loss of carbon of almost the same magnitude.

From these results one can derive some important information about the origin and composition of the ϵ-phase. The data in Table IX show that after annealing oxygen-rich samples at 1900°C/FC the ϵ-phase is the only precipitate present. Since this is a consequence of the lower carbon content at the end of the annealing treatment, obviously the ϵ-phase must have precipitated in a lower temperature region than the Cb_2C during cooling. It is also evident that the ϵ-phase is primarily a carbide and not an oxicarbide.

To conclude this chapter on internal oxidation of the columbium carbide D-43 an interesting observation shall be described which is deemed pertinent to any heat treatment of zirconium-bearing columbium alloys. It was suspected from the results of aging experiments in "medium" vacuum, as shown by Figure 1, that alloy D-43 in solution annealed condition is particularly sensitive to contamination effects on hardness.

To study this phenomenon more closely, a series of experiments was conducted in the following way: Samples of alloy D-43 were investigated in four different heat treated conditions:

1. as-received
2. as-received + 1hr/1400°C
3. solution annealed 1hr/1900°C/quenched
4. solution annealed 1hr/1900°C/fast-cooled.

* by Ledoux & Co.

The samples were ground, polished, and carefully cleaned. After annealing the samples for 1 hr at 1000°C in high vacuum (5×10^{-7} Torr) hardness and weight were measured. Oxygen was leaked into a closed, evacuated system containing the samples until a pressure of approximately 25×10^{-3} Torr was obtained. The glass system was then heated to 900°C. The absorption of oxygen by the samples was monitored by a thermocouple gage which showed a pressure drop to less than 1×10^{-3} Torr in about 10 minutes. To obtain variations in the amount of absorbed oxygen either the number of samples was varied or the contamination process was repeated. The contaminated samples were subsequently homogenized by annealing for 2 hrs. at 1000°C in high vacuum. The amount of absorbed oxygen was determined for each sample by weight measurements.

The hardness of the contaminated and homogenized samples is plotted versus absorbed oxygen content in Figure 18. There is a distinct difference between the hardness curves for solution annealed and soft-annealed samples. The solution annealed samples show a steep hardness increase up to an oxygen level of about 0.02 percent; above this concentration the hardness increases more slowly. The hardness of the soft-annealed samples increases continuously but much less pronounced. This hardness effect is not a surface phenomenon, since cross-sectional hardness was identical to that determined by surface measurements.

It was previously described that when oxygen-rich, as-received D-43 samples were annealed at 1000°C (see Table IX), the zirconium-rich MC-phase (Zr,Cb)C was decomposed and ZrO_2 and Cb_2C precipitated. Since ZrO_2 is shown to be stable at 1000°C, it should also be present in solution annealed and contaminated samples. X-ray analysis of extracted residues from such samples, however, did not reveal the presence of ZrO_2 precipitates.

The following interpretation is offered as explanation for the observed facts. In solution annealed samples, carbon exists in the form of Cb_2C, ϵ-carbide, and CbC, and zirconium is in homogeneous solid solution. Oxygen contamination of such a sample leads to precipitation of homogeneously distributed and extremely fine ZrO_2 particles which cause the observed strong hardening effect at 1000°C. In the soft-annealed D-43 alloy samples, however, zirconium is not in homogeneous solid solution but exists in form of the stable MC-phase (Zr,Cb)C. When the precipitates are decomposed and ZrO_2 is formed, it will exist as relatively large particles, since the diffusion rate of zirconium in D-43 should be relatively low at 1000°C. The non-homogeneous distribution and relatively large particle size of ZrO_2 will not exert a large effect on hardness. The fact that ZrO_2 was found in as-received, contaminated D-43 samples but not in solution annealed, contaminated samples may be explained by the extremely small size of the ZrO_2 precipitates in the latter samples, which elude detection by the experimental methods involved. A similar limit of detection was evident for the non-isothermally formed, homogeneous MC-phase in alloy D-31, as was described in Chapter 4.1.3.

4.3 THE ϵ-PHASE

After solution annealing a precipitate phase was found in both columbium alloys D-31 and D-43 which was designated as ϵ-phase. Since little attention has been given to this precipitate phase it is worthwhile to summarize the observations made during this investigation and further characterize its composition.

For ϵ-precipitates from quenched samples of both alloys the position and intensities of interference lines were identical. It is therefore assumed that the metallic alloying elements

W, Mo, Ti, and Zr are not of major importance for the formation of this phase. It was observed, however, that the interference line positions of the ϵ-phase in alloy D-31 were slightly shifted when the cooling rate was decreased after solution annealing. The reason for this line shift may be the high alloying element concentrations of titanium and molybdenum in alloy D-31 which become more influential on the lattice structure at lower cooling rates. The dependence of line position on cooling rate was much less for the ϵ-phase in alloy D-43. For simplicity the following discussion is primarily concerned with the ϵ-phase in alloy D-43.

The ϵ-phase precipitates from solid solution in a lower temperature range than the hexagonal Cb_2C (alloy D-43) or the cubic (Cb,Ti)C (alloy D-31). Since the precipitation reaction is extremely fast, it is difficult to determine the exact temperature range in which formation of ϵ occurs preferably. The experimental results of annealing tests with alloy D-31 suggest that ϵ-precipitation is possible below 1400°C (see Chapter 4.1.2). The preferable formation of ϵ-phase in this lower temperature region explains why faster cooling rates (i.e. higher degrees of supersaturation) promote ϵ-precipitation (see Chapter 4.2.2) and why ϵ-phase is the only precipitate found in fast-cooled (FC) D-43 samples with low carbon content (see Chapter 4.2.4).

The ϵ-phase was seen to transform during aging at temperatures around 1000°C into a phase with a lattice structure resembling that of Cb_2C (see Chapter 4.2.3, Table VII). Although it was not observed due to decomposition of Cb_2C and formation of (Zr,Cb)C, it is believed that ϵ-carbide can transform completely into Cb_2C with a concomitant change in composition. The ϵ-carbide is therefore not as stable as Cb_2C even in the temperature range in which the ϵ-phase is believed to precipitate. This behavior suggests that the lattice structure of ϵ-carbide is more easily formed from carbon-enriched matrix domains (e.g. by means of simple shear movements and/or by higher degrees of coherency) than the hexagonal Cb_2C structure. In the microstructure the ϵ-phase appears in form of thin platelets which are arranged in a type of Widmanstätten structure (see e.g. Figures 10c and 11a).

As mentioned before, it was possible to prepare samples of alloy D-43 which contained only ϵ-precipitates. The ϵ-phase of a sample, which had a carbon content of 0.0328 percent and an oxygen content of 0.0016 percent (see Chapter 4.2.4), was extracted and chemically analyzed:*)

columbium	75% ± 3%
tungsten	6.7%
zirconium	0.90%
carbon	6.83%
oxygen	5.90%

The high oxygen concentration of the precipitates disagrees with the chemical analysis of the bulk sample, for which the oxygen content was only 1/20 times the carbon content. It must be assumed that the extracted precipitates were enriched with oxygen by the extraction process. A similar result was reported by Chang (Reference 16) for analyses of precipitates extracted from columbium and molybdenum alloys. If the oxygen concentration is neglected, the composition of the ϵ-phase can be given as:

$$(Cb_{0.95}W_{0.04}Zr_{0.01})C_{0.67}$$

*) by Ledoux & Co.

This composition corresponds to a stoichiometry of about Cb_3C_2.

The lattice structure of this columbium carbide is not known. The x-ray diffraction pattern of the ϵ-carbide is given by the data in Table X and is illustrated by Figure 19. The diffraction patterns of Cb_2C and CbC are also shown in Figure 19 for comparison.

Investigating the carbide phases of columbium Lesser and Brauer (Reference 32) found a persistent diffraction line with a value of d = 2.28 Å samples of the two-phase region Cb_2C + CbC. They concluded that this line was produced by a third columbium carbide phase, which was called ξ, after they were able to isolate a similar ξ-carbide in the Ta-C system (Reference 33). The lattice structure of the ξ-tantalum carbide was not determined, but the chemical analysis gave a composition very close to the stoichiometric composition of Ta_3C_2. This composition seems to agree with that of the ϵ-carbide and there is a close similarity in the diffraction patterns which are reproduced in Figure 20.

Beside Cb_2C and CbC Pochon et al. (Reference 1) report also another columbium carbide which they called δ-CbC. This carbide was found as precipitate in columbium-carbon alloys with less than 0.15% and presumably formed during cooling. The δ-CbC appeared in the microstructure as needles arranged in a Widmanstätten pattern. Chemical analysis of the extracted precipitate gave a composition corresponding to $CbC_{0.976}$, which is close to the stoichiometry of CbC. The diffraction pattern of δ-CbC is not produced by a cubic (NaCl-type) lattice but was tentatively described as face-centered tetragonal. However, a comparison of the few reported diffraction data of δ-CbC with the diffraction pattern of the ϵ-carbide suggests that both precipitates have very similar lattice structures which cannot be described as f.c. tetragonal.

SECTION V

SUMMARY AND CONCLUSIONS

Solution and precipitation reactions were studied in the two commercial columbium alloys D-31 and D-43. The investigation yielded the following results and conclusions.

Annealing columbium alloys in conventional vacuum furnaces usually brings about a change in composition by contamination as well as by purification. These compositional changes may have a pronounced effect on the precipitation reactions and can be misleading in the interpretation of annealing results. Annealing alloys D-31 and D-43 in the temperature region of solid solution causes a decarburization. The loss of carbon was more pronounced in oxygen-enriched samples. The decarburization is doubtlessly caused by formation of carbon-monoxide and by the fact that the partial pressure of CO is always kept below the equilibrium pressure by the continuous pumping action. Annealing alloy D-43 at 1900°C reduced the oxygen content to about 0.002 percent. Annealing alloy D-31 at 1700°C, however, increased the oxygen content by 0.02 percent or more depending on the furnace pressure. When columbium alloys are annealed at lower temperatures (800° to 1500°C) in a vacuum of 1×10^{-6} to 1×10^{-5} Torr absorption of oxygen occurs and causes precipitation hardening effects which may be erroneously taken for aging reactions. The hardening effects are most pronounced in the zirconium-containing alloy D-43.

For samples of alloys D-31 and D-43 with low oxygen contents the thermodynamically stable precipitate phase is a monocarbide with NaCl-type lattice structure. The metallic components of this MC-phase are essentially shared by the alloying elements titanium or zirconium and columbium. The alloying elements molybdenum and tungsten seem to play a less prominent role in the formation of the MC-phase. In the temperature region below roughly 1200°C the monocarbide is titanium- or zirconium-rich for the two alloys, respectively. The ratios Ti/Cb and Zr/Cb, however, decrease at higher temperatures.

Complete solid solution of the MC-phase is achieved in alloy D-31 at 1580° ± 30°C and in alloy D-43 at 1670° ± 30°C. These solutioning temperatures correspond to a carbon content of approximately 0.09 percent. The lower solutioning temperature of alloy D-31 may be the influence of the high titanium content. Rapid grain growth is observed during annealing at temperatures where solid solution is achieved.

During cooling from the temperature region of solid solution columbium carbides precipitate in both alloys and appear in the microstructure as grain boundary precipitate and as platelet-like precipitates in the grain interior. These precipitates cause no essential hardness increase at room temperature. By varying the cooling rates it was possible to show that these columbium carbides precipitate during cooling and not during annealing as was assumed in earlier investigations. The rate of precipitation of the columbium carbides is so high that only in one instance it was possible to suppress the formation by quenching into an oil bath. It is this high rate of columbium carbide precipitation during cooling which prevents carbon supersaturation in columbium alloys and thus a controlled isothermal precipitation of stable MC-phase from solid solution.

Three different columbium carbides were found in both alloys after solution annealing:

(a) Columbium alloy D-31: A columbium-rich monocarbide (Cb,Ti)C, the cubic (NaCl-type) lattice structure of which was probably stabilized by a larger titanium content, precipitates during cooling in an upper temperature region below the temperature for solid solution.

In the next lower temperature region ϵ-carbide is formed. When the samples are quenched from the solid solution temperature region, additional precipitation of almost stoichiometric CbC was observed.

(b) Columbium alloy D-43: The sequence of precipitation during cooling from the temperature region of solid solution is analogous to that for alloy D-31, but with the difference that due to the low zirconium content of alloy D-43 hexagonal Cb_2C precipitates in the upper temperature range instead of the columbium-rich monocarbide (Cb,Ti)C. ϵ-carbide forms in the next lower temperature range, and after quenching almost stoichiometric CbC is found which appears in the microstructure in form of a very fine dispersion.

The columbium carbide phase designated as ϵ-carbide was found in both columbium alloys and precipitates during cooling in form of thin platelets. The crystal structure of the carbide phase was not determined but the chemical composition corresponds to Cb_3C_2. Precipitation of ϵ-carbide does preferably occur during comparatively fast cooling or in samples with low carbon contents. The nucleation and growth mechanisms appear to be more favorable at lower temperatures for the ϵ-carbide than for Cb_2C, although the ϵ-carbide is less stable than Cb_2C. By annealing at temperatures around 1000°C the ϵ-phase appears to transform into Cb_2C. The sequence of precipitation of the three columbium carbides Cb_2C, ϵ-carbide (Cb_3C_2), and CbC can be generalized in this way: the lower the temperature of formation, the higher is the carbon content of the carbide precipitate. A similar phenomenon is known for cementite precipitation in steels.

A strong hardness increase was observed after annealing alloy D-31 in the temperature region of increasing MC-phase solutioning. The columbium carbides found in these samples by metallographic and x-ray diffraction methods are too coarse to be responsible for the hardening effect. By indirect evidence it was concluded that the hardness increase is caused by a very fine precipitation of stable MC-phase which is formed during cooling and quenching and cannot be detected metallographically or by x-ray powder methods. Such hardness increase is neither observed in a sample with much lower titanium content nor in alloy D-43.

After one-hour aging treatments of solution-annealed and quenched samples a pronounced age hardening peak is found at 400°C for alloy D-43 and at 450°C for alloy D-31. The reason for the age-hardening peak was not determined with certainty. This anomaly is believed to be caused by either precipitation or transformation of a less stable columbium carbide.

Overaging of the titanium-rich MC-phase, which was formed in alloy D-31 during cooling after solution annealing, occurs at 1000°C and higher temperatures and causes a hardness decrease. The ϵ-carbide and subsequently the cubic, columbium-rich (Cb,Ti)C dissolve during aging at and above 1200°C in favor of additional MC-phase precipitation, which,however, has no effect on hardness.

The precipitation reactions during aging at higher temperatures are very similar for both alloys. In addition, a transformation of ϵ-carbide, probably into Cb_2C, was found in alloy D-43 prior to MC-precipitation. Age-hardening by MC-phase precipitation was also not detected in alloy D-43.

Oxide phases were not found in alloy D-31, although the oxygen content was purposely increased. On the other hand it was determined that the titanium-rich MC-phase dissolves large amounts of oxygen. Titanium-rich oxicarbide is therefore more stable than pure oxides and carbides. It is thought that the titanium-rich MC-phase, which forms during cooling after solution annealing, dissolves also a large amount of oxygen.

Contrary to alloy D-31, oxide phases were found in alloy D-43. ZrO_2 is a stable oxide phase in the temperature region between 1000° and at least 1400°C. It was shown that the zirconium-rich MC-phase in alloy D-43 decomposed to ZrO_2 and Cb_2C, when the samples were charged with oxygen. It is concluded that the stability of ZrO_2 is comparatively high and that the zirconium-rich MC-phase does not dissolve appreciable amounts of oxygen.

The formation of ZrO_2 and Cb_2C by internal oxidation of (Zr,Cb)C produces only a modest hardness increase. Oxidation of Zr at 1000°C, when it is in homogeneous solid solution, however, causes a large hardness increase. It is believed that the ZrO_2-precipitation in the latter case consists of a fine particle size of less than 500 to 1000 Å, since it was not detected by surface replica electron micrographs.

The results of this investigation lead to the conclusion that controlled age-hardening by precipitation of stable carbides from supersaturated solid solution is not feasible in columbium alloys. It may be possible to derive some benefit for high temperature strength from strain-induced carbide precipitation, but the rapid grain growth, which can hardly be avoided during solution annealing, may impair the margin of benefit for current columbium alloys.

SECTION VI

REFERENCES

1. M. L. Pochon, C. R. McKinsey, R. A. Perkins and W. D. Forgeng, Reactive Metals, p. 327, AIME Conf. Proc., Interscience Publ., New York, 1959.

2. R. P. Elliott, Trans. ASM, 53, 1961, p. 13 - 28.

3. H. Kimura and Y. Sasaki, Trans. Japan. Inst. Metals, 2, 1961, p. 98 - 104.

4. R. T. Begley, W. N. Platte, A. I. Lewis, R. L. Ammon, "Development of Niobium-Base Alloys", WADC-TR 57-344, Pt. V, 1961.

5. W. M. Albrecht and W. D. Goode, Battelle Memorial Institute Report No. BMI-1360.

6. R. P. Elliott and S. Komjathy, Columbium Metallurgy, p. 367, Interscience Publ. New York, 1961.

7. J. Cost and C. Wert, Acta Met., 11, 1963, p. 321.

8. E. deLamotte, Y. Huang and C. Altstetter, ML-TDR-64-134, 1964.

9. E. Gebhard, E. Fromm and D. Jakob, Z. Metallkunde, 55, 1964, p. 423 - 431.

10. C. Ang and C. Wert, Trans. AIME, 197, 1953, p. 1032.

11. R. P. Elliott, "Columbium-Oxygen System", ASM Preprint, No. 143, 1959.

12. D. O. Hobson, "Aging Phenomena in Columbium-Base Alloys", p. 325, High Temperature Materials II, Interscience Publ., New York, 1963.

13. A. C. Barber and P. H. Morton, "A Study of the Cb-Zr-C and Cb-Zr-O Systems", Imperial Metal Industries, Birmingham, United Kingdom, 93rd AIME Annual Conference, New York, Feb. 1964.

14. E. deLamotte, Y. C. Huang and C. J. Altstetter, "Equilibrium Solutions of Nitrogen in Niobium-Base Alloys", University of ILLinois, AFML-Technical Report 65-164, Aug. 1965.

15. J. R. Stewart, W. Liebermann and G. H. Rowe, "Recovery and Recrystallization of Columbium-1,0% Zirconium Alloy", p. 407, Columbium Metallurgy, Interscience Publishers, New York, 1961.

16. W. H. Chang, "A Study of the Influence of Heat Treatment on Microstructure and Properties of Refractory Alloys", General Electric Co., ASD-TDR-62-211, Feb. 1962.

17. R. T. Begley, R. L. Ammon and R. Stickler, "Development of Niobium-Base Alloys", Westinghouse Electric Corp., WADC-TR-57-344, Pt. VI, Feb. 1963.

18. R. T. Begley, J. L. Godshall and R. Stickler, "Precipitation Hardening Columbium-Hafnium-Nitrogen Alloys", 5. Plansee Seminar, Reutte/Tirol, June 1964, Preprint Nr. 20.

REFERENCES (CONT'D)

19. R. E. Yount and D. L. Keller, "The Structural Stability of Welds in Columbium Alloys", General Electric Co., ML-TDR-64-210, June 1964.

20. H. Inouye, "The Contamination of Refractory Metals in Vacua Below 10^{-6} Torr", AIME Technical Conf. on Applied Aspects of Refractory Metals, Los Angeles, Calif., Dec. 1963.

21. R. T. Begley, "Developments of Niobium-Base Alloys", Westinghouse Electric Corp., WADC-TR-57-344, Nov. 1957.

22. R. W. Hall and R. H. Titran, "Creep Properties of Columbium Alloys in Very High Vacuum", AIME Technical Conference on Applied Aspects of Refractory Metals, Los Angeles, Calif., Dec. 1963.

23. R. T. Roche, "The Effect of Degree of Vacuum on the Slow-Bend Creep Behavior of Columbium-0,6% Zirconium at 1000°C", AIME Technical Conference on Applied Aspects of Refractory Metals, Los Angeles, Calif., Dec. 1963.

24. F. B. Cuff, Jr., "Research to Determine the Composition of Dispersed Phases in Refractory Metals", Advanced Metals Research Corp., ASD Technical Report 62-7, Pt. I, 1962.

25. H. F. Beeghly, Anal. Chem. 24, 1713, 1952.

26. P. Schwartzkopf and R. Kieffer, Refractory Hard Metals, The MacMillan Company, New York, 1953.

27. I. Cadoff, J. P. Nielson and E. Miller, Plansee Seminar Proc. 1955, 50.

28. C. P. Kempter, E. K. Storms and R. J. Fries, J. Chem. Phys., 33, (1960), 1873-4.

29. G. Brauer, Z Anorg. Chemie, 248, (1941), 1.

30. J. T. Norton and A. L. Mowry, Trans. AIME 185, (1949), 133.

31. T. K. Roche, "Aging of Columbium Alloy D-43", AIME Conference, Chicago, Ill., 14 - 18 Feb. 1965.

32. G. Brauer and R. Lesser, Z. Metallkunde, 50, (1959), p. 8 - 10.

33. R. Lesser and G. Brauer, Z. Metallkunde, 49, (1958), p. 622.

34. F. Bollenrath, unpublished results.

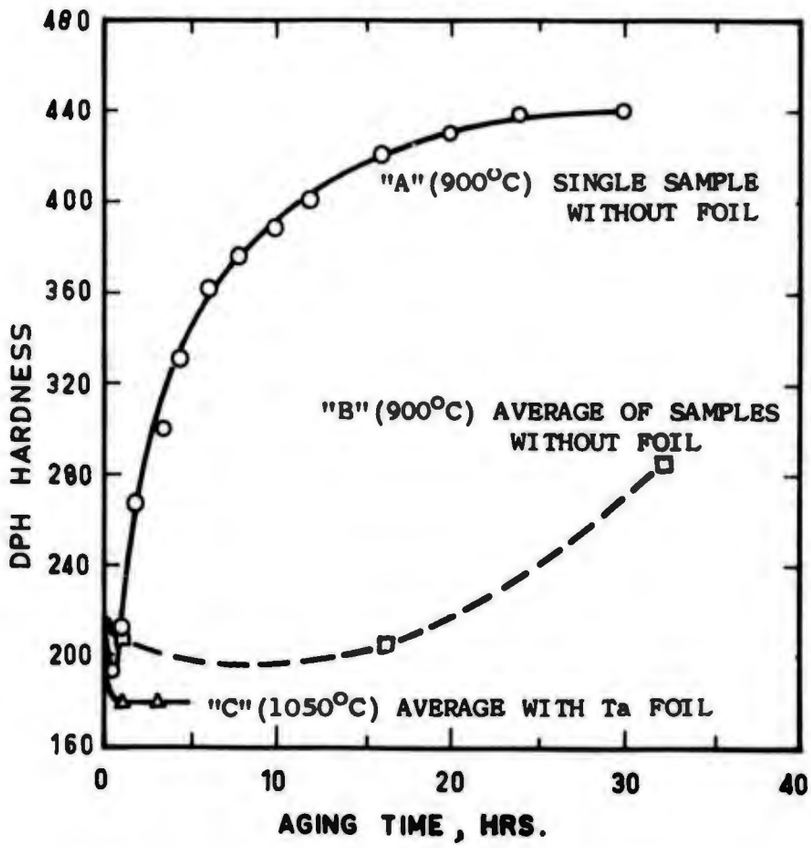

Figure 1. Alloy D-43. Effects of Contamination on Room Temperature Hardness of Solution Annealed Samples. (1hr/1900°C/OQ) During Aging in a Vacuum of 1×10^{-5} Torr.

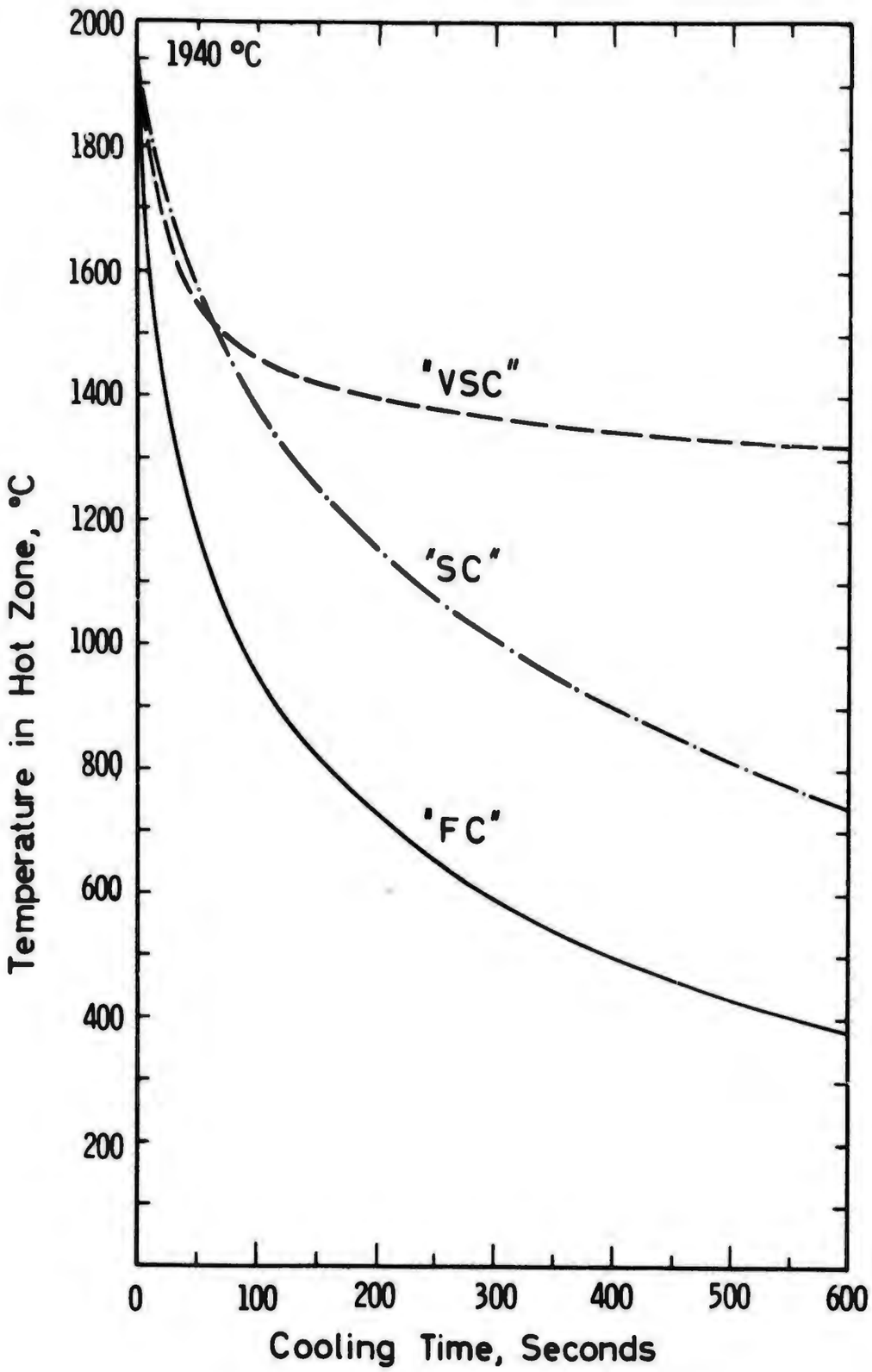

Figure 2. Cooling Curves for Annealing Treatments in Radiation Cooled Vacuum Furnace "A".

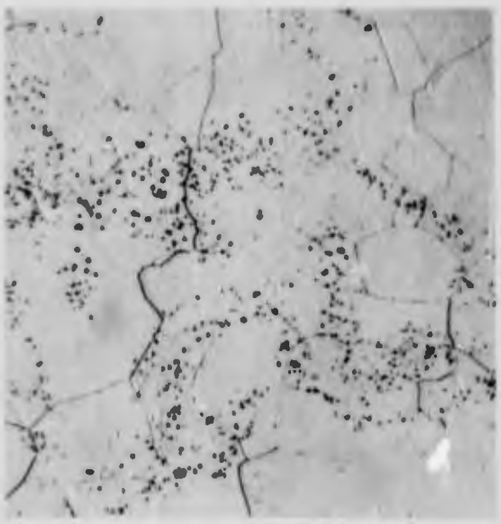

a. As-received, 800x

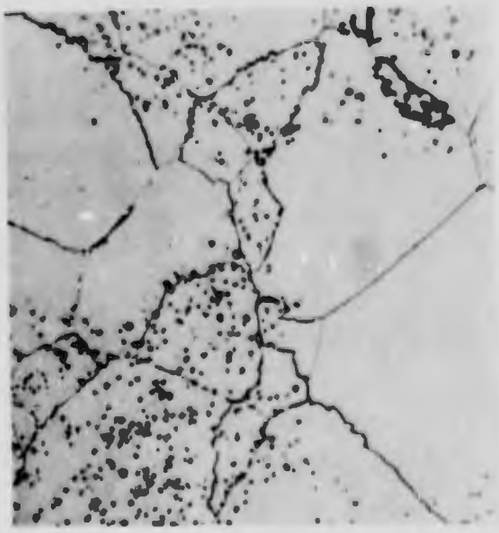

b. 1hr/1500°C/FC, 800x

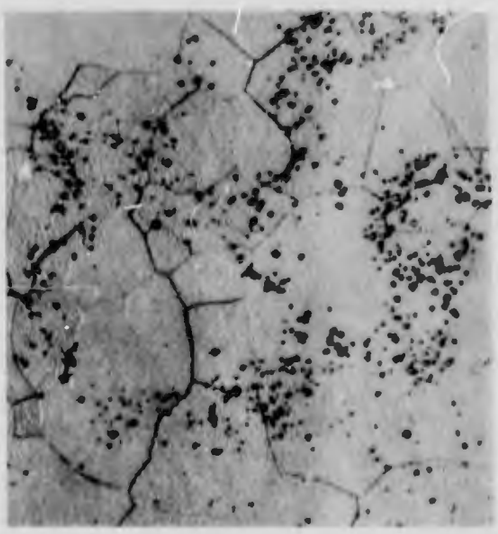

c. 1hr/1500°C/OQ, 800x

Figure 3a-g. Alloy D-31. Effects of Annealing Temperature and Cooling Rate on Microstructure.

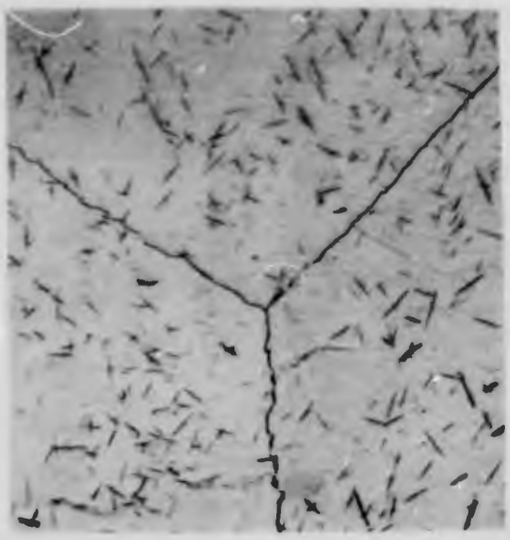

d. 1hr/1600°C/FC, 800x

e. 1hr/1600°C/OQ, 800x

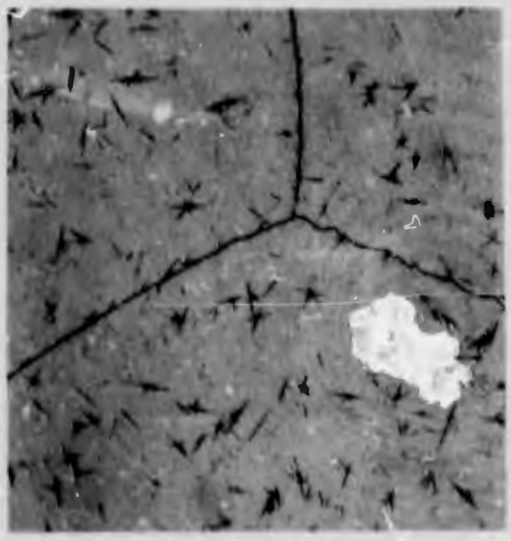

f. 1hr/1700°C/FC, 800x

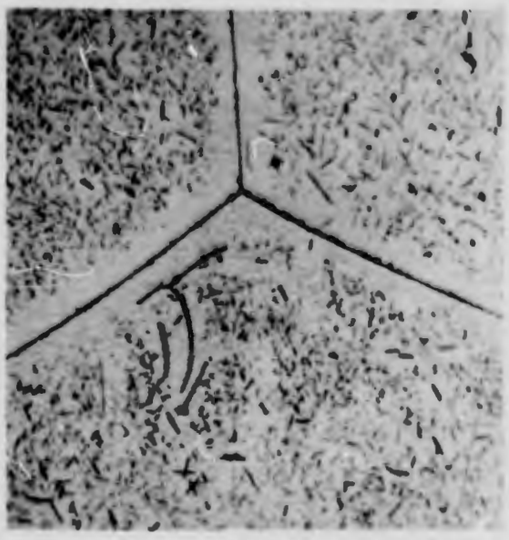

g. 1hr/1700°C/OQ, 800x

Figure 3. (Cont'd)

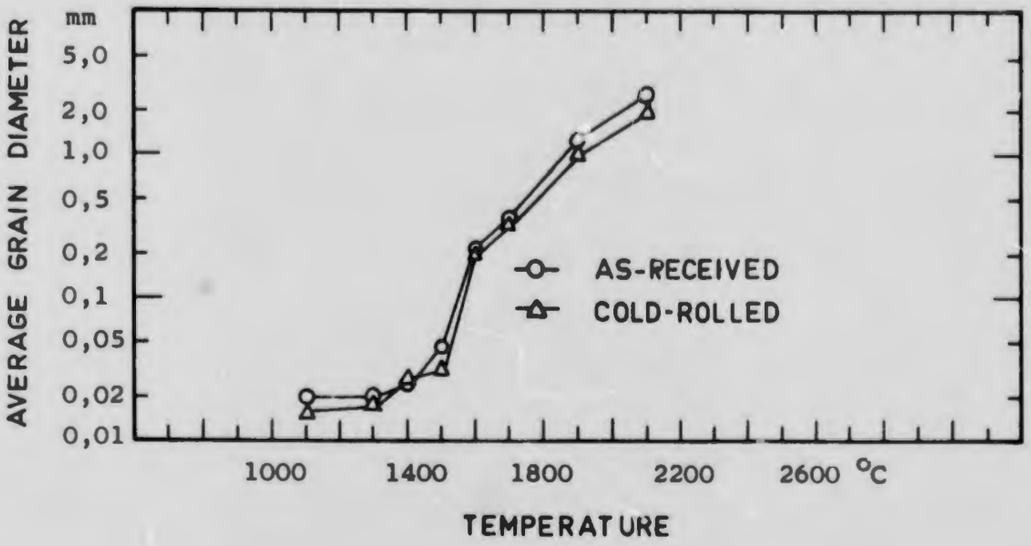

Figure 4. Alloy D-31. Average Grain Size After Annealing One Hour at Various Temperatures.

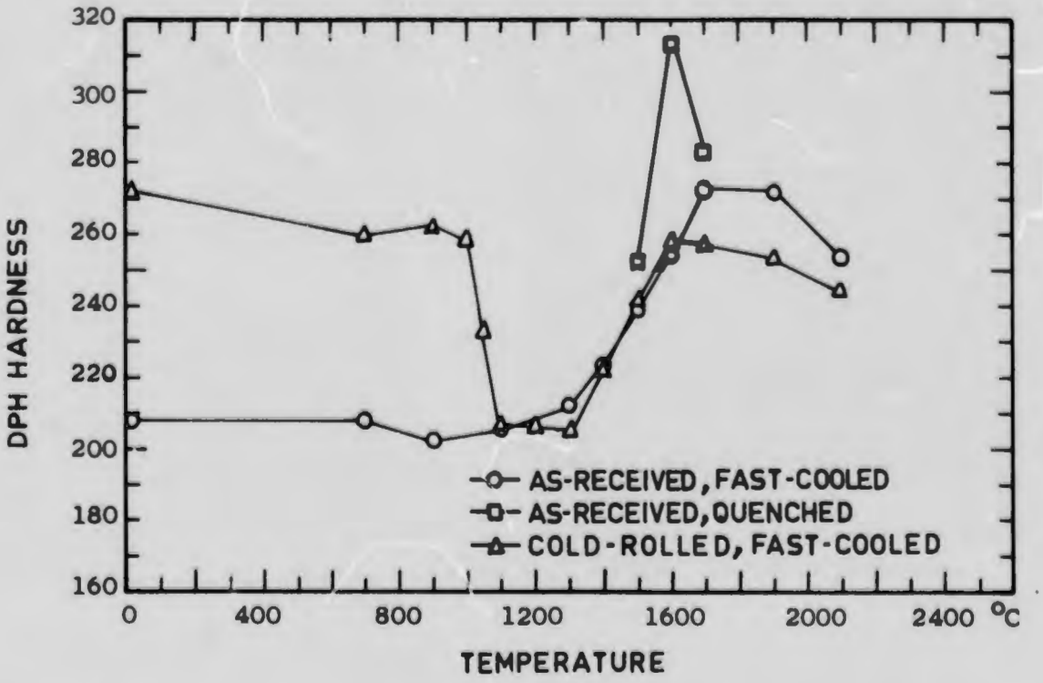

Figure 5. Alloy D-31. Hardness of As-received and of Cold-Rolled Samples After One-Hour Annealing Treatments

a. Quenched in oil (OQ)

b. Fast radiation cooling (FC)

c. Slow radiation cooling (SC)

Figure 6a-c. Alloy D-31 Effect of Cooling Rate on Microstructure After Solution-Annealing 1hr/1700°C.

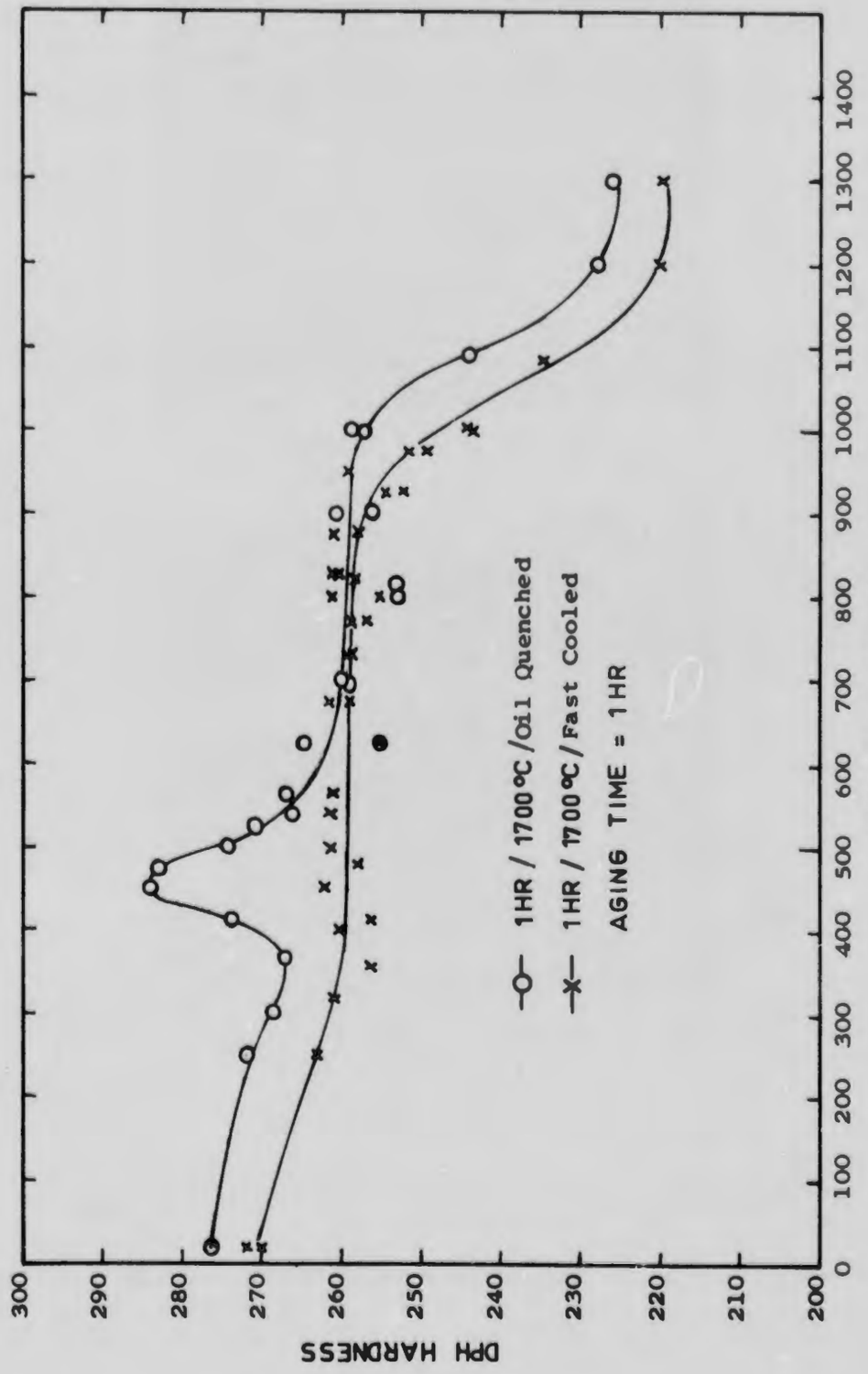

Figure 7. Alloy D-31. Effects of One-Hour Aging Treatments on Room Temperature Hardness.

a. 1hr/1700°C/FC + 1hr/1200°C

b. 1hr/1700°C/FC + 1hr/1300°C, 800x

Figure 8a-b. Alloy D-31. Microstructure After Solution Annealing and Aging.

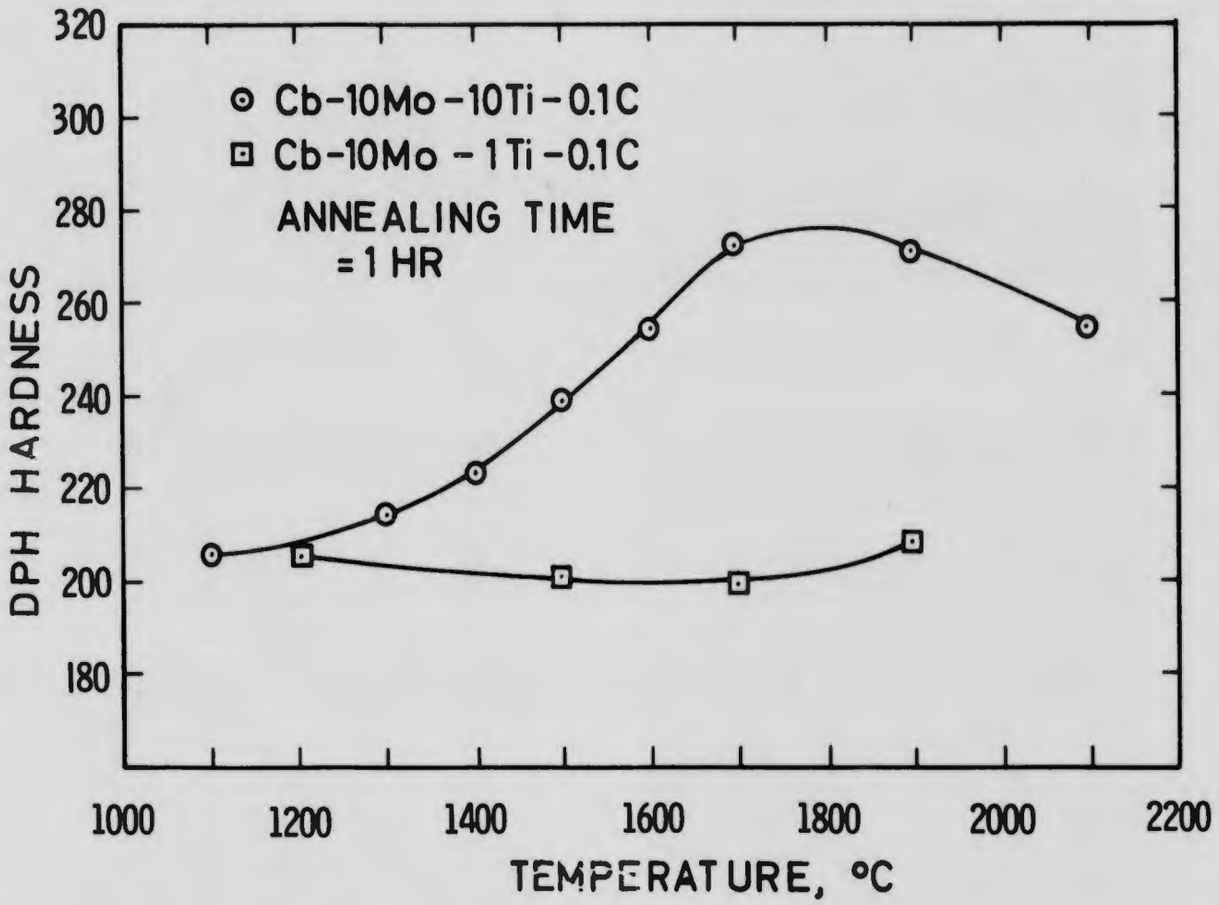

Figure 9. A Comparison of Hardness of Alloys D-31 and Cb-10Mo-1Ti-0.1C After Annealing and Fast Cooling

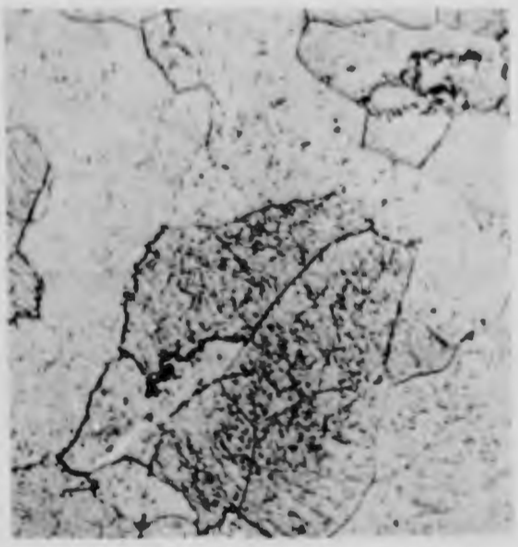

a. As-received, 800x

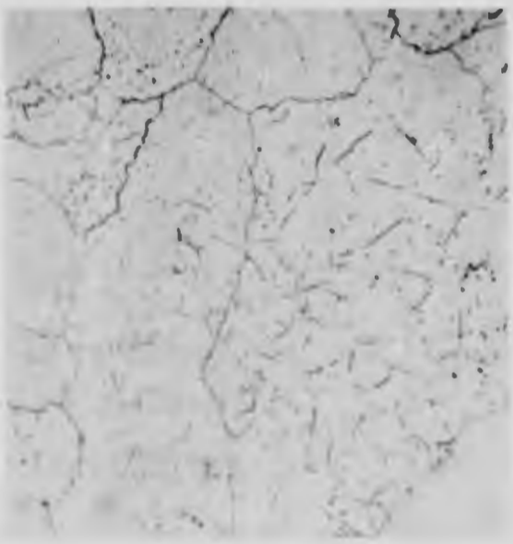

b. 1hr/1600 C/FC, 800x

c. 1hr/1700°C/FC, 800x

d. 1hr/2000°C/FC, Overetched, 800x

Figure 10a-d. Alloy D-43. Effects of Annealing Temperature on Microstructure.

a. Fast Radiation Cooling (FC)

b. Slow Radiation Cooling (SC)

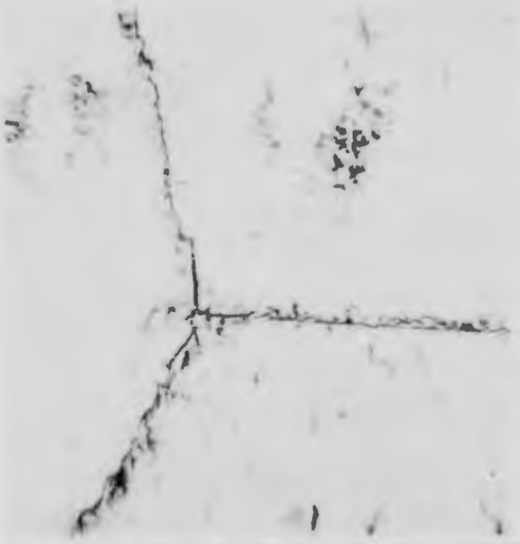

c. Very Slow Radiation Cooling (VSC)

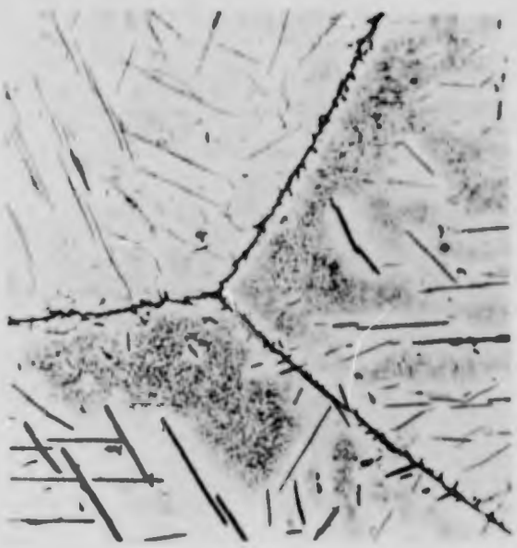

d. Quenched in Oil (OQ)

Figure 11a-d, Alloy D-43. Effects of Cooling Rate on Microstructure After Solution Annealing 1hr/1900°C, 800x

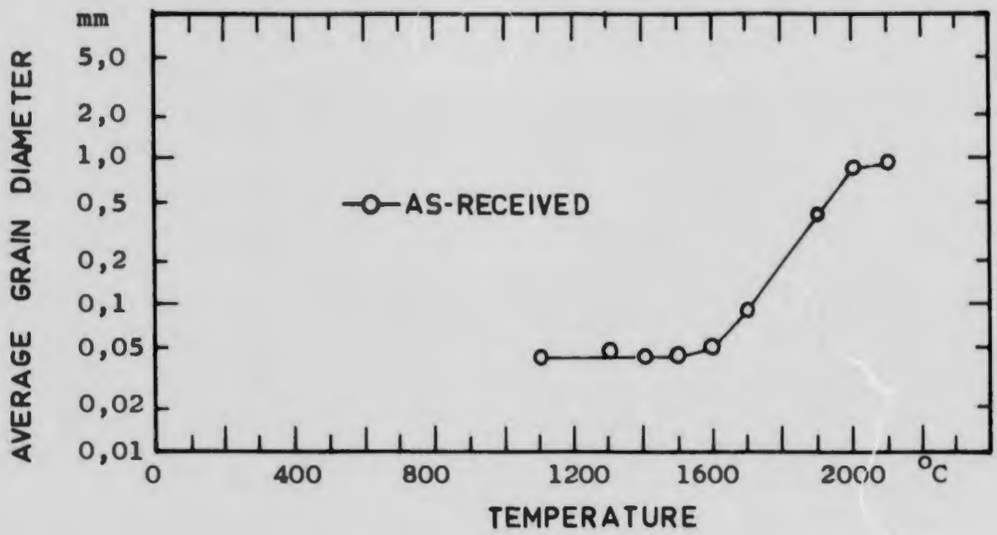

Figure 12. Average Grain Size After Annealing for One Hour.

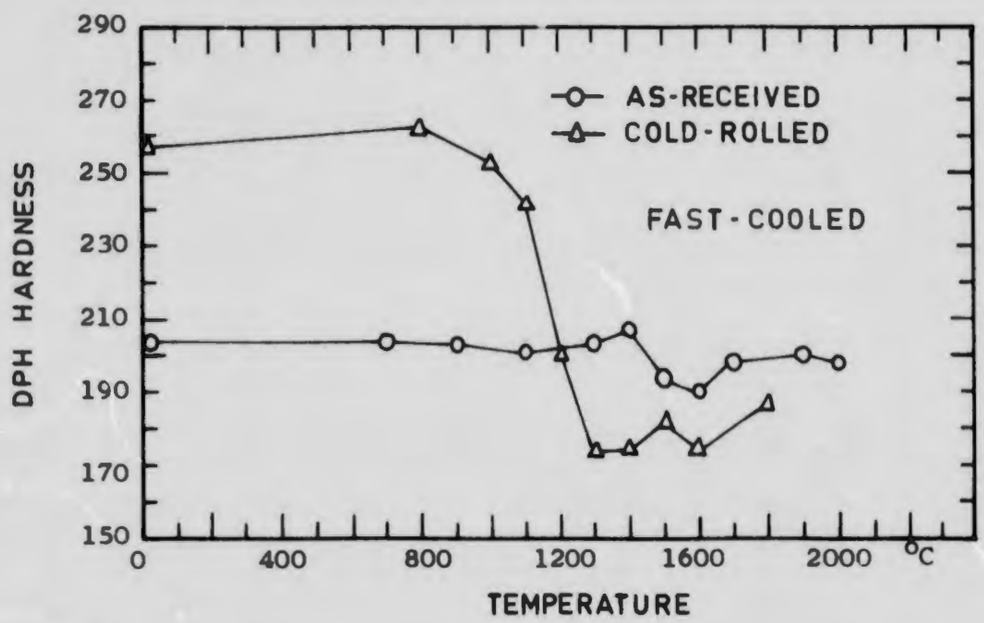

Figure 13. Alloy D-43. Hardness of Samples After One-Hour Annealing Treatments.

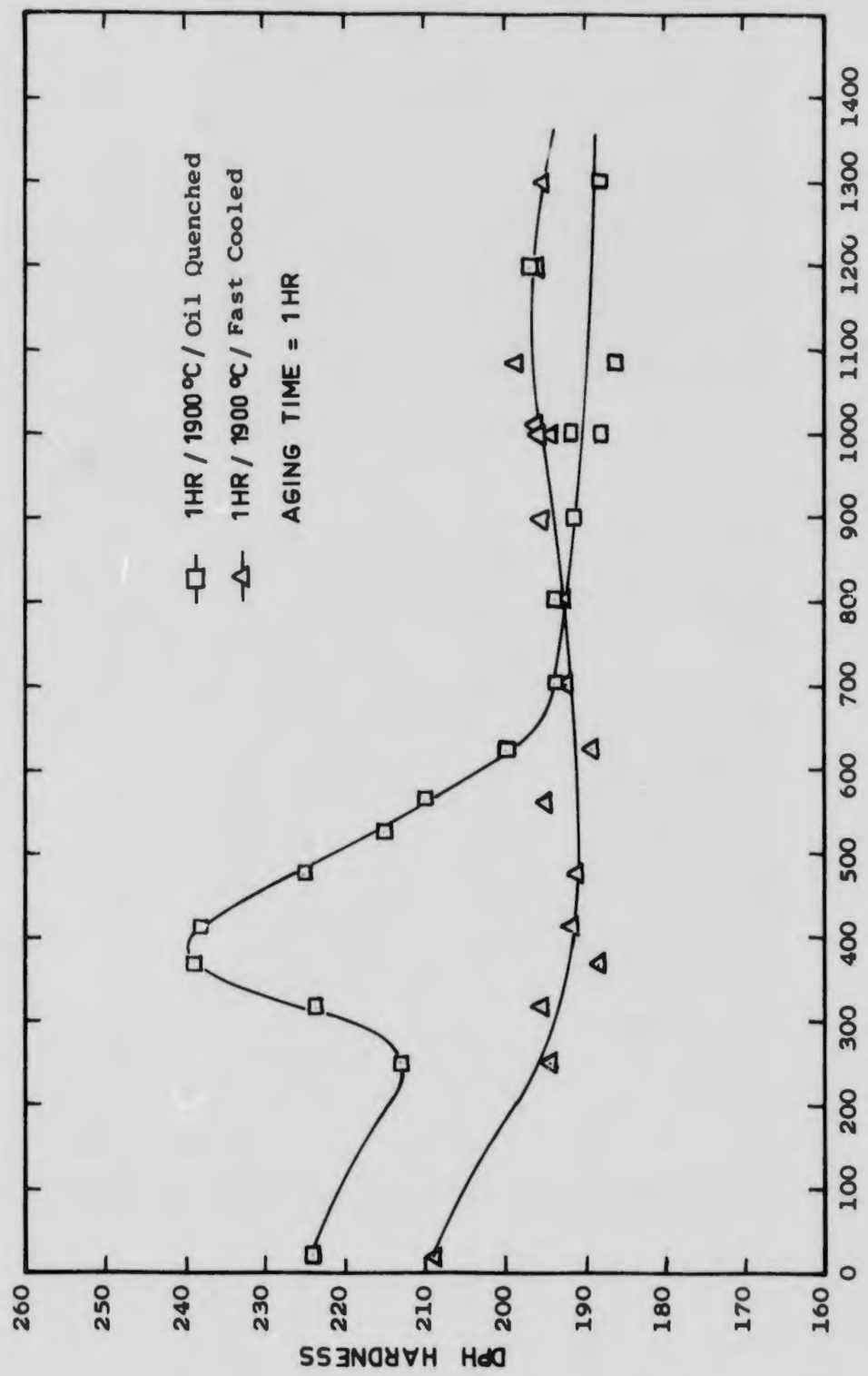

Figure 14. Alloy D-43. Effects of Aging Treatments on Room Temperature Hardness of Solution Annealed Samples

a. 1hr/1900°C/OQ + 1hr/624°C, 800x

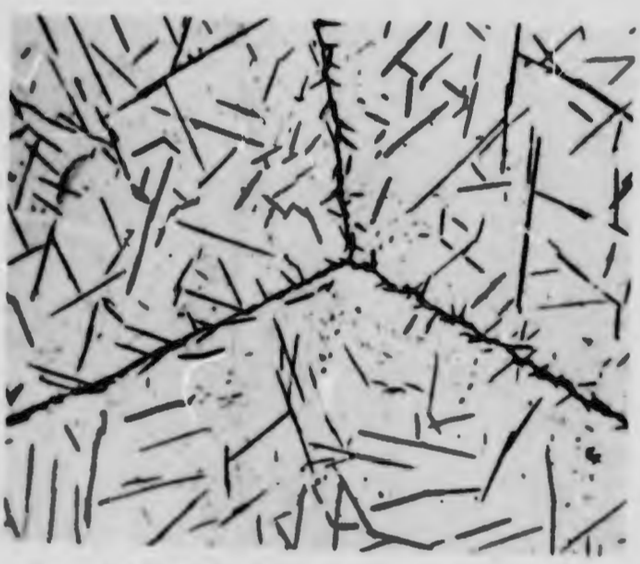

b. 1hr/1900°C/OQ + 10hrs/1000°C, 800x

Figure 15a-b. Effects of Aging on Microstructure of Solution Annealed and Oil-quenched Samples

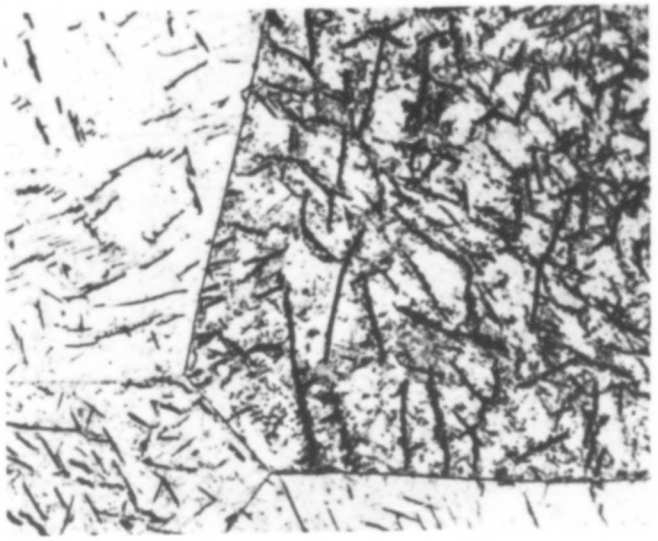

a. Optical Micrograph, 800x

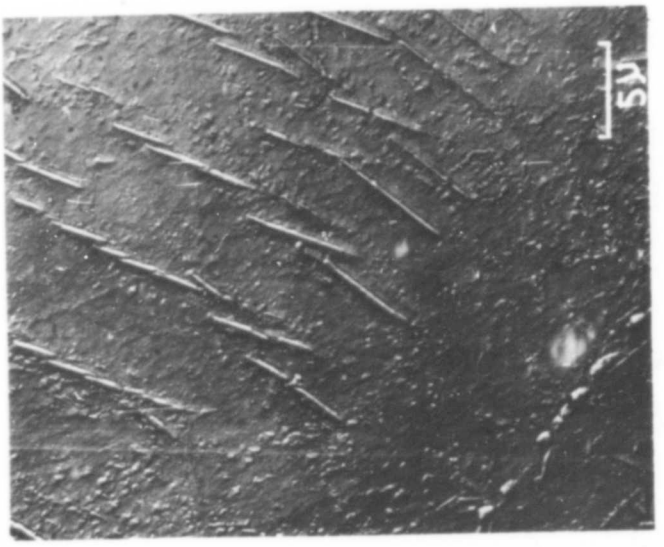

b. Electron Micrograph, 2,500x

Figure 16a-b. Alloy D-43. Microstructures of a Solution Annealed and Aged Sample (1hr/1900°C/OQ + 1hr/1300°C).

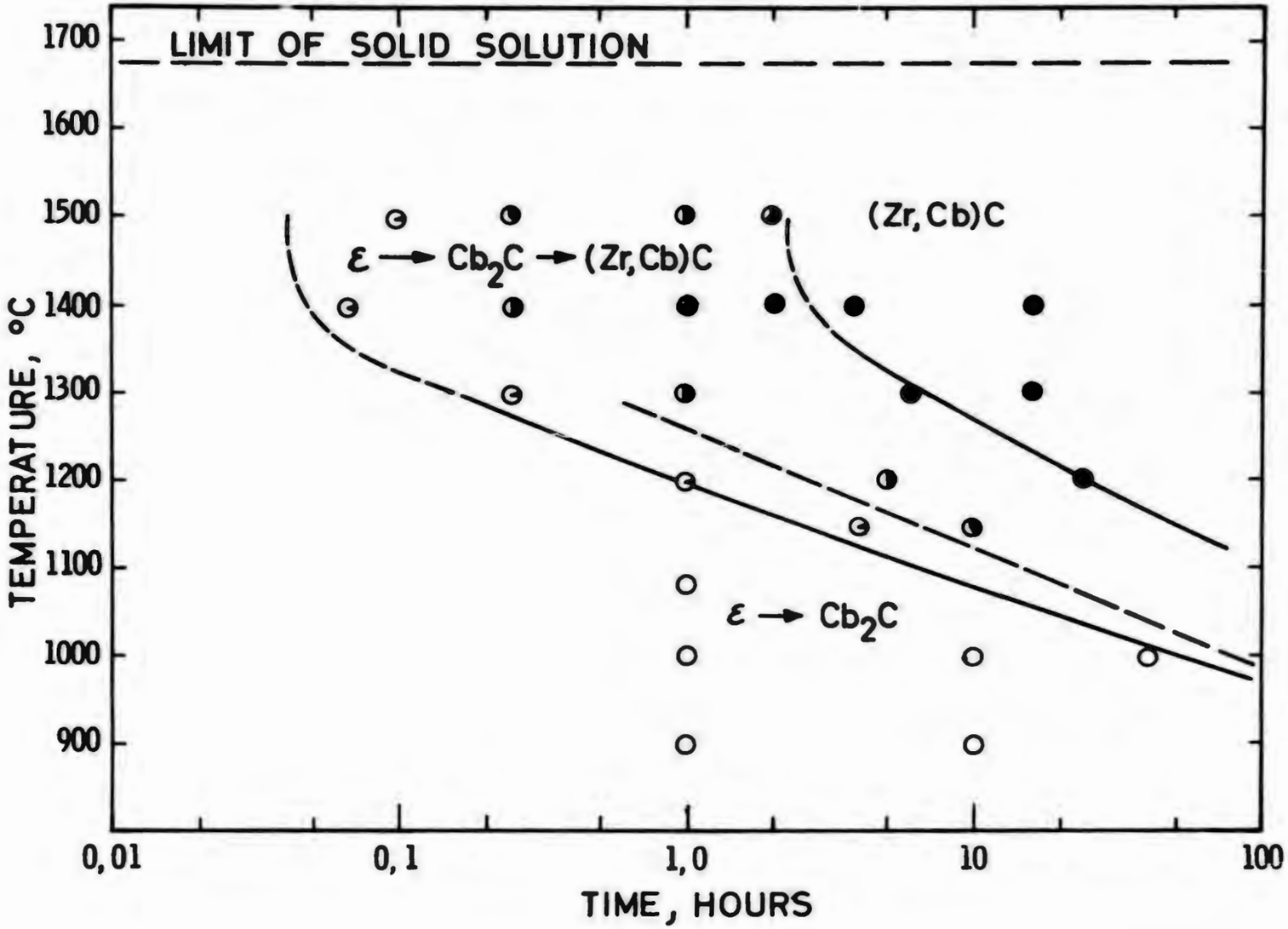

Figure 17a. Alloy D-43. MC-Phase Precipitation During Aging of Solution Annealed and Oil-quenched Samples (1hr/1900° C/OQ).

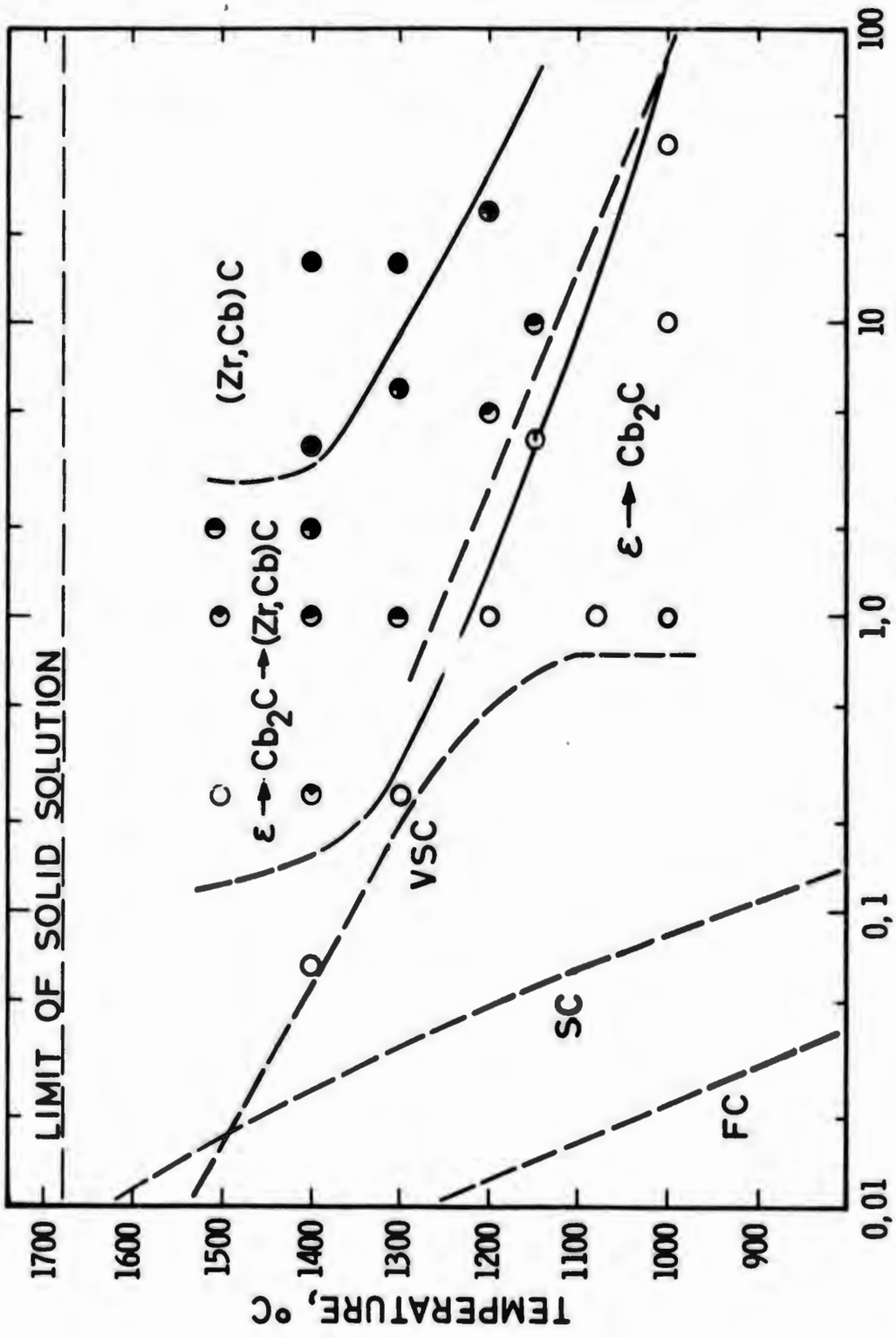

Figure 17b. Alloy D-43. MC-Phase Precipitation During Aging of Solution Annealed and Fast-Cooled Samples (1hr/1900°C/FC).

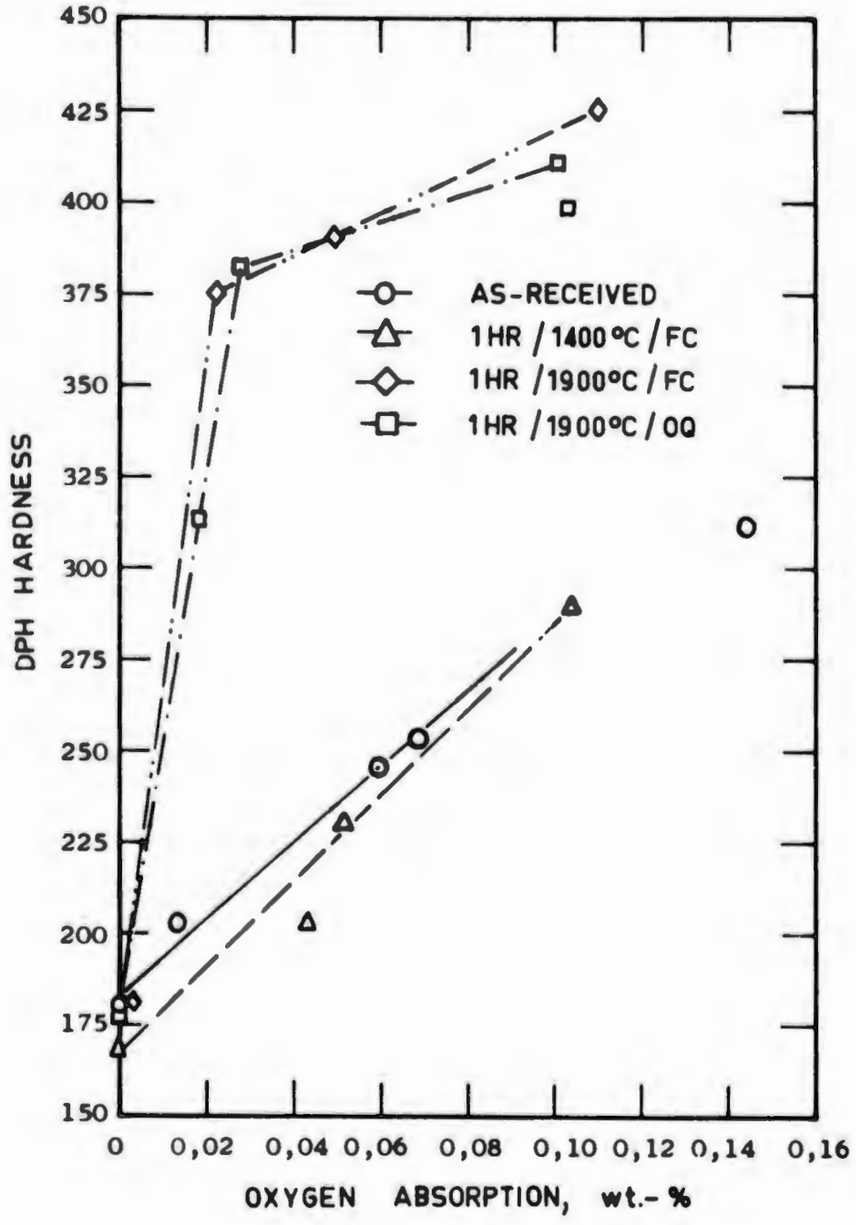

Figure 18. Alloy D-43. Influence of Oxygen Contamination on Hardness of Samples Contaminated at 900°C and Homogenized 1 hr at 1000°C.

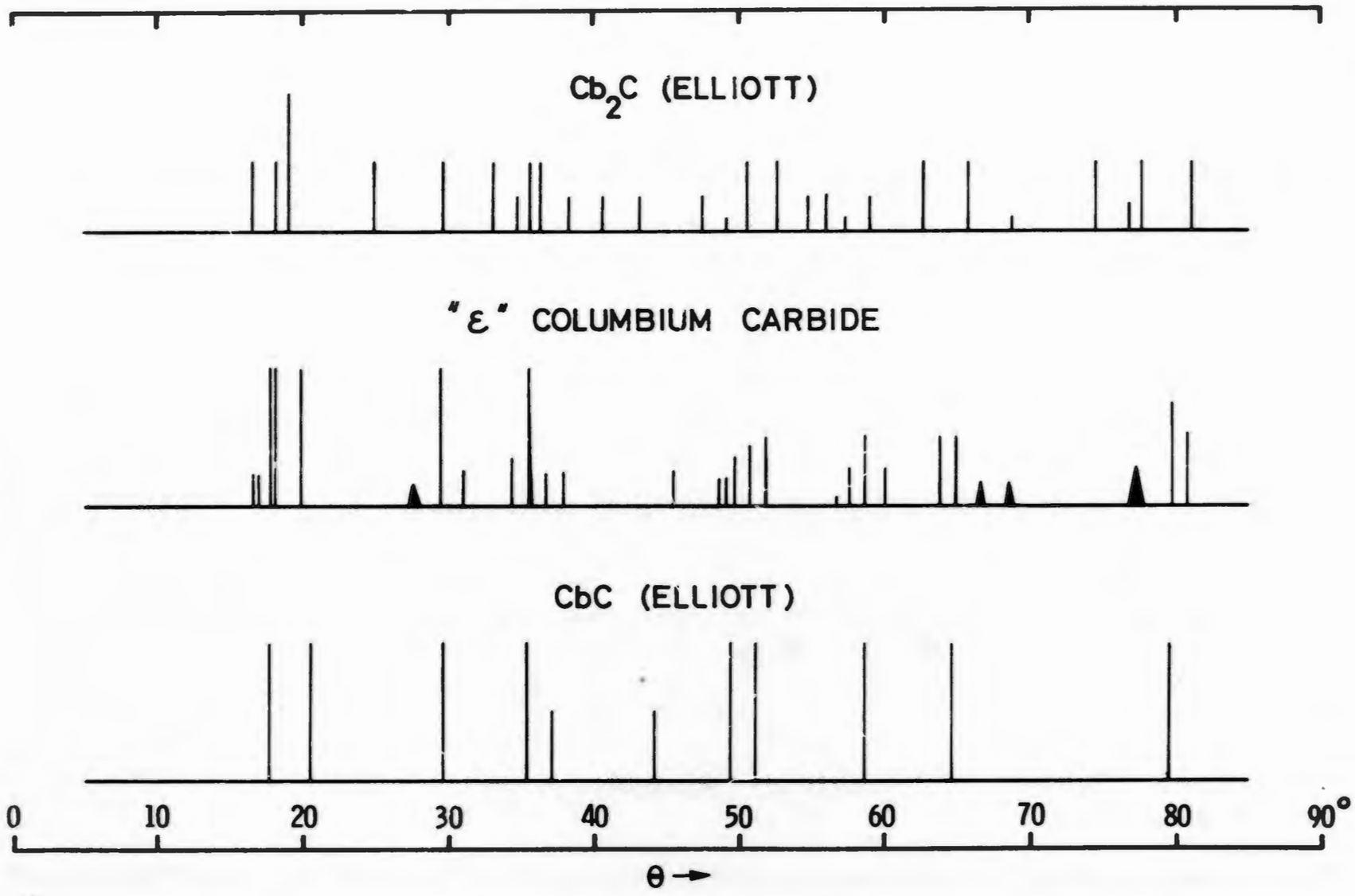

Figure 19. X-ray Diffraction Patterns of the Columbium Carbides Cb_2C, CbC, and ϵ -Carbide.

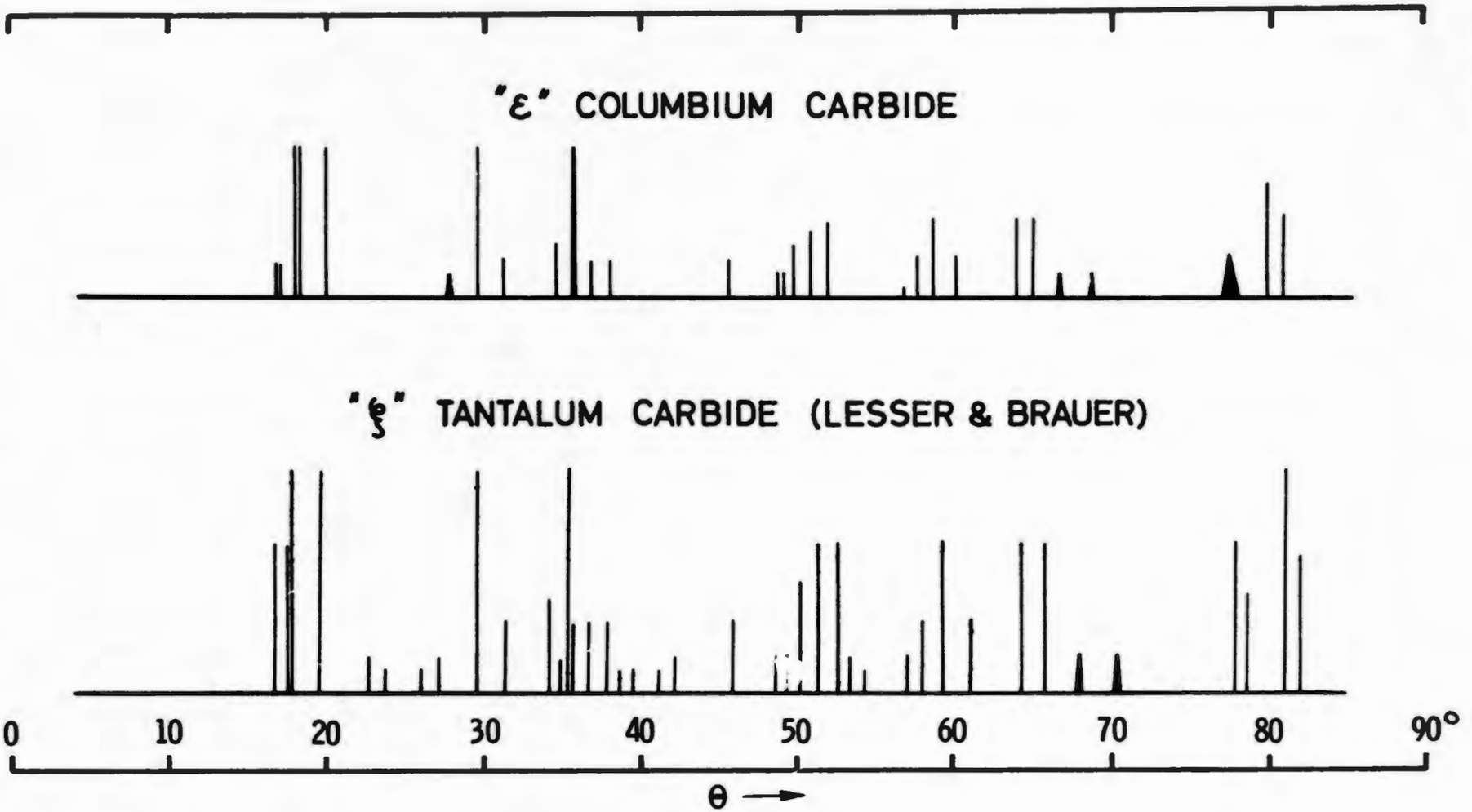

Figure 20. X-ray Diffraction Patterns of ϵ-Columbium Carbide and ξ-Tantalum Carbide

TABLE I

INTERSTITIAL CONTENT OF COLUMBIUM ALLOY D-31
AFTER SOLUTION ANNEALING

	As-received analysis	Furnace "A" 1 hr/1700°C/FC $p \approx 1 \times 10^{-5}$ Torr	Furnace "B" 1 hr/1700°C/OQ $p \approx 1 \times 10^{-4}$ Torr
Carbon	0.094%	0.0650%	0.0500%
Oxygen	0.017%	0.0366%	0.0503%
Nitrogen	0.013%	0.0108%	0.0109%

Chemical analysis by Ledoux & Co.

TABLE II

PRECIPITATES IN COLUMBIUM ALLOY D-31
AFTER VARIOUS HEAT TREATMENTS

Heat Treatment	Precipitates	Intensity	Lattice Structure	Lattice Parameter, Å
as-received	(Ti,Cb)(C,O,N)	s	cubic	a = 4.322
1hr/1400°C/FC	(Ti,Cb)(C,O,N)	s	cubic	a = 4.328
	ϵ	vvw	x	x
1hr/1500°C/FC	(Ti,Cb)(C,O,N)	s	cubic	a = 4.342
	ϵ	w	x	x
1hr/1500°C/OQ	(Ti,Cb)(C,O,N)	s	cubic	a = 4.320
1hr/1600°C/FC	(Cb,Ti)(C,O)	s	cubic	a = 4.388
	"CbC"	m	cubic	a = 4.42
	ϵ	w	x	x
1hr/1700°C/FC	(Cb,Ti)(C,O)	s	cubic	a = 4.398
	ϵ	m	x	x
1hr/1800°C/FC	(Cb,Ti)(C,O)	s	cubic	a = 4.398
	ϵ	m	x	x
1hr/1700°C/OQ	ϵ	s	x	x
	"CbC"	s	cubic	a = 4.47
	(Cb,Ti)(C,O)	m-w	cubic	a = 4.36
	others	vvw		
1hr/1700°C/FC	(Cb,Ti)(C,O)	s	cubic	a = 4.39
+ 1hr/1200°C	(Ti,Cb)(C,O)	w	cubic	a = 4.34
	ϵ	w	x	x
1hr/1700°C/FC	(Ti,Cb)(C,O)	s	cubic	a = 4.34
+ 16hrs/1200°C	matrix	vw		
1hr/1700°C/FC	(Ti,Cb)(C,O)	s	cubic	a = 4.35
+ 1hr/1300°C	(Cb,Ti)(C,O)	m	cubic	a = 4.39
	ϵ	vw	x	x

s = strong, m = medium strong, w = weak, vw = very weak
x = lattice structure of ϵ-phase was not determined
FC = fast-cooled, OQ = oil-quenched

TABLE III

PRECIPITATES IN OXYGEN-RICH SAMPLE OF ALLOY D-31
AFTER VARIOUS HEAT TREATMENTS

Heat Treatment	Precipitates	Intensity	Lattice Structure	Parameter, Å
16hrs/1200°C	(Ti,Cb)(C,O) (Ti,Cb)(C,O,N)	s m	cubic cubic	a = 4.292 a = 4.232
16hrs/1200°C + 10hrs/1300°C	(Ti,Cb)(C,O)	s	cubic	a = 4.300
1hr/1700°C/FC	ϵ - phase (Cb,Ti)(C,O) Cb_2C	s w vvw	x cubic hexagonal	x a = 4.39 n.d.

s = strong, m = medium, w = weak
x = lattice structure of ϵ-phase was not determined

TABLE IV

HARDNESS VALUES OF ALLOY D-31 WITH DIFFERENT OXYGEN CONTENTS
AFTER SOLUTION ANNEALING 1 HR/1700°C/FC

Oxygen content before sol.-anneal, %	0.017	0.029	0.043	0.052	0.080
Oxygen content after *) solution anneal, %	0.036	-.-	-.-	0.028	-.-
Carbon content *) after solution anneal, %	0.065	-.-	-.-	0.045	-.-
Hardness, DPH	270	294	275	274	301

*) Analysis by Ledoux & Co.

TABLE V

PRECIPITATES IN ALLOY D-43 AFTER VARIOUS HEAT TREATMENTS

Heat Treatment	Precipitates	Intensity	Lattice Structure	Lattice Parameter, Å
As-received	(Cb,Zr)C	s	cubic	a = 4.51
	(Zr,Cb)C	m-s	cubic	a = 4.60
	Cb_2C	m	hexagonal	a/c = 3.14/ 5.00
1hr/1400°C/FC	(Cb,Zr)C	s	cubic	a = 4.51
	(Zr,Cb)C	s	cubic	a = 4.60
	Cb_2C	vw	hexagonal	not determ.
16hrs/1400°C/ FC	(Zr,Cb)C	s	cubic	a = 4.60
	(Cb,Zr) C	m-s	cubic	a = 4.51
	Cb_2C	w	hexagonal	not determ.
	ZrO_2	vw	tetragonal	not determ.
1hr/1600°C/FC	(Cb,Zr)C	s	cubic	a = 4.51
	(Zr,Cb)C	w-m	cubic	a = 4.60
	Cb_2C	s	hexagonal	a/c = 3.14/ 5.00
1hr/1650°C/OQ	(Cb,Zr)C	s	cubic	a = 4.49
	€	s	x	x
	Cb_2C	m	hexagonal	a/c = 3.12/ 4.99
1hr/1800°C/FC	€	s	x	x
	Cb_2C	s	hexagonal	a/c = 3.12/ 4.99
1hr/1900°C/FC	€	s	x	x
	Cb_2C	m-s	hexagonal	a/c = 3.12/ 4.99
1hr/2000°C/FC	€	s	x	x
	Cb_2C	m	hexagonal	a/c = 3.12/ 4.99
1hr/1900°C/OQ	€	s	x	x
	Cb_2C	w	hexagonal	a/c = 3.12/ 4.99
	CbC	w	cubic	a = 4.46
1hr/1900°C/SC	€	s	x	x
	Cb_2C	s	hexagonal	a/c = 3.12/ 4.99
1-1/4hr/1900°C/ VSC	Cb_2C	s	hexagonal	a/c = 3.12/ 4.99
	€	m	x	x

OQ = oil-quenched, FC = fast-cooled, SC = slow-cooled, VSC = very-slowly-cooled (see also figure 2).

TABLE VI

INTERSTITIAL CONTENT OF COLUMBIUM ALLOY D-43
AFTER SOLUTION ANNEALING

	As-received Analysis	Furnace "A" 1 hr/1900°C/FC $p \approx 1 \times 10^{-5}$ Torr	Furnace "B" 1 hr/1900°C/OQ $p \approx 1 \times 10^{-4}$ Torr
Carbon	0.0970%	0.0920%	0.0840%
Oxygen	0.0067%	0.0020%	0.0025%
Nitrogen	0.0025%	0.0024%	0.0037%

Chemical analysis by Ledoux & Co.

TABLE VII

X-RAY DIFFRACTION DATA FOR THE TRANSFORMATION OF ϵ -CARBIDE DURING AGING AT 900° AND 1000°C

1hr/1900°C quenched	1hr 700°C	1hr 900°C	10hrs 900°C	1hr 1000°C	10hrs 1000°C	40hrs 1000°C	hk.l	Cb_2C *) d_o, Å	I_o
2.698w	2.693w	2.696m	2.696m	2.697s	2.694s	2.683m	10.0	2.682	m
2.642w	2.639w	diff.							
2.512s	2.503vs	2.496s	2.479s	2.487vs	2.480vs	2.477s	00.2	2.474	m
2.478s	2.477vs	diff.	2.396m	2.400s	2.391s	2.385s	10.1	2.361	s
2.276s	2.274vs	diff.	2.345m	2.339s	2.355s	2.343s			
2.051vwd	2.052vwd								
1.826tr	1.830vw			1.829vw	1.831w	1.829tr	10.2	1.824	m
1.661vw	1.662vw								
1.563s	1.564vs	1.565s	1.562s	1.564vs	1.561vs	1.560s	11.0	1.558	m
1.492w	1.496w	1.491tr		1.503tr					
			1.429tr	1.415vw	1.418vw	1.415vw	10.3	1.411	m
1.361w	1.362w	1.368vw	1.394tr	1.393vw	1.399vw	1.397vw			
			1.351vw	1.352vw	1.351vw	1.349vw	20.0	1.349	w
1.327s	1.328vs	1.327s	1.323s	1.324vs	1.323vs	1.322s	11.2	1.321	m
1.289w	1.2902w	1.296w	1.297w	1.301w	1.300w	1.298w	20.1	1.302	m
1.256w	1.259w	1.250w	1.245w	1.245w	1.2435w	1.243w	00.4	1.240	w
							20.2	1.186	w
	1.138vw						10.4	1.127	w
1.0808vw	1.0827vw			1.0559vw	1.0553vw	1.055vw			
1.0273vw	1.0293vw	1.0322vw	1.0387tr	1.0402vw	1.0427vw	1.040vw	20.3	1.046	w
1.0207vw	1.0230vw	1.0243vw	1.0230vw	1.0242vw	1.0222vw	1.0216vw	21.0	1.021	vw
1.0108w	1.0111m	1.0094md	1.0061wd	1.0052md	1.0045md				
0.9955w	0.9954m	0.9981m	0.9988wd	1.0011md	1.0005md	diff., m	21.1	0.9998	m
0.9799m	0.9805m	0.9777m	0.9727m	0.9738m	0.9726m	0.9723md	11.4	0.9713	m
							21.2	0.9444	w
	0.9222tr			0.938wd			10.5	0.9318	w
0.9130w	0.9121w			0.926vwd			20.4	0.9173	vw
0.9036m	0.9044m	0.9049m	0.9032w	0.90345m	0.9033m	0.9020md	30.0	0.9002	w
0.889w	0.8904w			0.8760wd	0.8746wd	diff., w	21.3	0.8688	m
0.8591m	0.8595m		0.8654vw	0.8671wd	0.8664wd				
0.850m	0.850m	0.8507md	0.8490m	0.8496m	0.8490md	diff.,m	30.2	0.8463	m

*) according to R. P. Elliott, Trans. ASM, 53 (1961), 13 - 28.
s = strong; m = medium; w = weak; vw = very weak; tr = trace; d = diffuse

TABLE VIII

EFFECT OF ANNEALING TEMPERATURE ON LATTICE PARAMETER OF (Zr,Cb)C IN COLUMBIUM ALLOY D-43

Temperature °C	Annealing time, hrs	Lattice parameter, Å	Zr/Cb *)
1200	24	4.58	1.9
1400	2	4.56	1.2
1500	2	4.53	0.9

*) Maximum values; calculated from data of Norton and Mowry [30]

TABLE IX

PRECIPITATES IN OXYGEN-RICH SAMPLES OF ALLOY D-43 IN VARIOUS HEAT TREATED CONDITIONS *)

Oxygen Content & Heat Treatment	Precipitates	Intensity	Lattice Structure	Lattice Parameter
0.14% O 2hrs/1000°C	(Cb,Zr)C	s	cubic	4.51
	Cb_2C	s	hexagonal	3.13/4.98
	ZrO_2	m	tetragonal	not determ.
	ZrO_2	w	monoclinic	not determ.
0.026% O 16hrs/1400°C	(Zr,Cb)C	s	cubic	4.60
	Cb_2C	w	hexagonal	3.13/4.95
	ZrO_2	w	tetragonal	not determ.
	ZrO_2	w	monoclinic	not determ.
0.023% O 1hr/1900°C/FC	ϵ	s	x	x
	Cb_2C	vw	hexagonal	not determ.
0.035% O 1hr/1900°C/FC	ϵ	s	x	x
0.059% O 1hr/1900°C/FC	ϵ	s	x	x

*) Oxygen was added in the as-received condition.
x = Lattice structure and parameter of ϵ -phase was not determined.

TABLE X

X-RAY DIFFRACTION DATA OF THE ϵ -PHASE

d_o, Å	I_o	d_o, Å	I_o
2.683	w	1.0269	vw, diff.
2.644	w	1.0222	vw, diff.
2.498	s	1.0101	m
2.471	s	0.9955	m
2.269	s	0.9793	m
1.663	vvw, diff.	0.9132	w
1.561	s	0.9028	m
1.488	w, diff.	0.8887	w, diff.
1.362	w	0.8590	m, diff.
1.324	s	0.8503	m, diff.
1.288	w	0.8378	vvw
1.256	w	0.8269	vvw
1.0791	vw, diff.	0.7825	m, diff.

UNCLASSIFIED

Security Classification

DOCUMENT CONTROL DATA · R&D

(Security classification of title, body of abstract and indexing annotation must be entered when the overall report is classified)

1 ORIGINATING ACTIVITY (Corporate author)	2a REPORT SECURITY CLASSIFICATION
Air Force Materials Laboratory, Research and Technology Division, Air Force Systems Command, Wright-Patterson Air Force Base, Ohio	UNCLASSIFIED
	2b GROUP

3 REPORT TITLE

INVESTIGATION OF PRECIPITATES IN TWO CARBON-CONTAINING COLUMBIUM-BASE ALLOYS

4 DESCRIPTIVE NOTES (Type of report and inclusive dates)

5 AUTHOR(S) (Last name, first name, initial)

F. Ostermann

F. Bollenrath

6 REPORT DATE	7a TOTAL NO. OF PAGES	7b NO OF REFS
December 1966	65	34

8a CONTRACT OR GRANT NO.	9a ORIGINATOR'S REPORT NUMBER(S)
b. PROJECT NO 7351	AFML-TR-66-259
c. Task No. 735106	9b. OTHER REPORT NO(S) (Any other numbers that may be assigned this report)
d	

10 AVAILABILITY/LIMITATION NOTICES

Distribution of this document is unlimited

11. SUPPLEMENTARY NOTES	12. SPONSORING MILITARY ACTIVITY
	Air Force Materials Laboratory Research and Technology Division Wright-Patterson Air Force Base, Ohio

13. ABSTRACT

The precipitates in the commercial columbium alloys D-31 and D-43 were investigated after various heat treatments. The titanium-rich and zirconium-rich monocarbides are the only stable precipitate phases in alloys D-31 and D-43, respectively. The temperatures for complete solid solution are 1600°C for alloy D-31 and 1700°C for alloy D-43 corresponding to a carbon content of about 0.09 wt.-%. Non-equilibrium columbium carbides precipitate even during quenching from solid solution, so that no appreciable carbon supersaturation can be achieved in columbium alloys. During aging, the stable monocarbides form at the expense of the non-equilibrium columbium carbides but not from solid solution. Therefore, age-hardening caused by stable MC-phase precipitation does not occur. The effect of oxygen on carbide precipitates was investigated by increasing the oxygen concentration of the alloys on purpose. Oxygen behaved differently in both alloys with respect to precipitate phases. A columbium carbide phase with unknown lattice structure but a composition corresponding approximately to Cb_3C_2 was found in both alloys after suitable heat treatments.

DD FORM 1 JAN 64 1473

UNCLASSIFIED

Security Classification

14 KEY WORDS	LINK A		LINK B		LINK C	
	ROLE	WT	ROLE	WT	ROLE	WT
1. Columbium-Base Alloys						
2. Solution Annealing						
3. Heat Treatment						
4. Carbide Precipitation						
5. Precipitation Strengthening						
6. Internal Oxidation						

INSTRUCTIONS

1. ORIGINATING ACTIVITY: Enter the name and address of the contractor, subcontractor, grantee, Department of Defense activity or other organization *(corporate author)* issuing the report.

2a. REPORT SECURITY CLASSIFICATION: Enter the overall security classification of the report. Indicate whether "Restricted Data" is included. Marking is to be in accordance with appropriate security regulations.

2b. GROUP: Automatic downgrading is specified in DoD Directive 5200.10 and Armed Forces Industrial Manual. Enter the group number. Also, when applicable, show that optional markings have been used for Group 3 and Group 4 as authorized.

3. REPORT TITLE: Enter the complete report title in all capital letters. Titles in all cases should be unclassified. If a meaningful title cannot be selected without classification, show title classification in all capitals in parenthesis immediately following the title.

4. DESCRIPTIVE NOTES: If appropriate, enter the type of report, e.g., interim, progress, summary, annual, or final. Give the inclusive dates when a specific reporting period is covered.

5. AUTHOR(S): Enter the name(s) of author(s) as shown on or in the report. Enter last name, first name, middle initial. If military, show rank and branch of service. The name of the principal author is an absolute minimum requirement.

6. REPORT DATE: Enter the date of the report as day, month, year; or month, year. If more than one date appears on the report, use date of publication.

7a. TOTAL NUMBER OF PAGES: The total page count should follow normal pagination procedures, i.e., enter the number of pages containing information.

7b. NUMBER OF REFERENCES: Enter the total number of references cited in the report.

8a. CONTRACT OR GRANT NUMBER: If appropriate, enter the applicable number of the contract or grant under which the report was written.

8b, 8c, & 8d. PROJECT NUMBER: Enter the appropriate military department identification, such as project number, subproject number, system numbers, task number, etc.

9a. ORIGINATOR'S REPORT NUMBER(S): Enter the official report number by which the document will be identified and controlled by the originating activity. This number must be unique to this report.

9b. OTHER REPORT NUMBER(S): If the report has been assigned any other report numbers *(either by the originator or by the sponsor)*, also enter this number(s).

10. AVAILABILITY/LIMITATION NOTICES: Enter any limitations on further dissemination of the report, other than those imposed by security classification, using standard statements such as:

(1) "Qualified requesters may obtain copies of this report from DDC."

(2) "Foreign announcement and dissemination of this report by DDC is not authorized."

(3) "U. S. Government agencies may obtain copies of this report directly from DDC. Other qualified DDC users shall request through _____."

(4) "U. S. military agencies may obtain copies of this report directly from DDC. Other qualified users shall request through _____."

(5) "All distribution of this report is controlled. Qualified DDC users shall request through _____."

If the report has been furnished to the Office of Technical Services, Department of Commerce, for sale to the public, indicate this fact and enter the price, if known.

11. SUPPLEMENTARY NOTES: Use for additional explanatory notes.

12. SPONSORING MILITARY ACTIVITY: Enter the name of the departmental project office or laboratory sponsoring *(paying for)* the research and development. Include address.

13. ABSTRACT: Enter an abstract giving a brief and factual summary of the document indicative of the report, even though it may also appear elsewhere in the body of the technical report. If additional space is required, a continuation sheet shall be attached.

It is highly desirable that the abstract of classified reports be unclassified. Each paragraph of the abstract shall end with an indication of the military security classification of the information in the paragraph, represented as *(TS), (S), (C), or (U)*.

There is no limitation on the length of the abstract. However, the suggested length is from 150 to 225 words.

14. KEY WORDS: Key words are technically meaningful terms or short phrases that characterize a report and may be used as index entries for cataloging the report. Key words must be selected so that no security classification is required. Identifiers, such as equipment model designation, trade name, military project code name, geographic location, may be used as key words but will be followed by an indication of technical context. The assignment of links, rules, and weights is optional.